BMC Genomics

RESEARCH

Open Access

Enhancing sweet sorghum emergence and stress resilience in saline-alkaline soils through ABA seed priming: insights into hormonal and metabolic reprogramming

Jianfeng Yang[1,2†], Wenlan Zhang[1,2†], Tianyu Wang[1,2], Jiawei Xu[1,3], Jinjing Wang[1,2], Jiahao Huang[1,2], Yingpeng Sun[1,3], Yu Ni[4] and Yanjun Guo[1,2,3*]

Abstract

Sweet sorghum (*Sorghum bicolor* Moench) seedling emergence and growth are significantly impeded by physical soil crusts (PSCs) in saline-alkaline soils. Abscisic acid (ABA) is a potent seed priming agent known for modulating plant physiological and metabolic responses under salinity stress. However, the influence of ABA priming on seedling emergence in PSCs remains unclear. This study conducted both pot and field experiment to examine the effects of ABA priming on enhancing seedling emergence under PSC conditions. ABA priming altered the balance of at least 24 endogenous phytohormones, including abscisic acid, jasmonic acid, gibberellins, ethylene, auxins, and cytokinins. Additionally, it reprogrammed starch and sucrose metabolism, resulting in the differential expression of genes encoding key enzymes such as AMY, BAM, and INV, which are crucial for converting complex sugars into readily available energy sources, thereby supporting seedling growth. Furthermore, 52 differentially expressed metabolites (DEMs) of flavonoids were identified in germinating seedlings, including 15 anthocyanins, 3 flavones, 7 flavonols, 6 isoflavones, 7 flavanones, and 14 other flavonoids. Genetic and metabolic co-expression network analysis, along with flavonoid biosynthesis pathway exploration, revealed that the biosynthesis of 17 key DEMs—including liquiritigenin, apigenin, kaempferide, syringetin, phloretin, formononetin, dihydrokaempferol, and xanthohumol—was regulated by 10 differentially expressed genes (DEGs) associated with flavonoid biosynthesis. These DEGs encoded 7 enzymes critical for this pathway, including chalcone synthase, shikimate O-hydroxycinnamoyltransferase, bifunctional dihydroflavonol 4-reductase, naringenin 7-O-methyltransferase, and anthocyanidin reductase. This regulation, along with reduced levels of superoxide anion (O_2^-) and malondialdehyde and increased antioxidant enzyme activities, suggested that flavonoids played a vital role in mitigating oxidative stress. These findings demonstrate that ABA priming can effectively enhance sweet sorghum seedling emergence in PSCs by accelerating emergence and boosting stress resistance.

Keywords Abscisic acid (ABA), Physical soil crusts (PSCs), Saline-alkaline soil, Seedling emergence, Sweet sorghum

†Jianfeng Yang and Wenlan Zhang contributed equally to this work.

*Correspondence:
Yanjun Guo
qhgyj@qau.edu.cn

Full list of author information is available at the end of the article

Introduction

Sweet sorghum (*Sorghum bicolor* Moench), a crucial forage and biofuel energy crop, boasts wide distribution in saline-alkaline soils owing to its robust resilience against drought, salt, and nutrient deficiencies [1, 2]. However, sorghum seedling emergence faces challenges in saline-alkaline soils [3], where the presence of unstable loamy soils with low organic matter content and degraded soils resulting from intensive land use foster the development of physical soil crusts (PSCs) [4]. Therefore, enhancing seedling emergence in crusted soil is imperative for achieving optimal harvest yields in such soils. Abscisic acid (ABA), as one of the important seed priming agents, has been shown to be effective in mediating plant physiological and metabolic responses that are sensitive to salinity stress [5]. However, whether and how ABA priming influences seedling emergence in PSCs is still unclear.

Generally, ABA levels are typically high in dormant seeds, inhibiting germination processes. As germination progresses, ABA levels gradually decrease, breaking seed dormancy and initiating germination processes. A decline in ABA levels allows for the expression of genes involved in radicle elongation and seedling establishment [6]. By exposing seeds to ABA during priming, more ABA would enter the seeds before germination. Such an increase might disrupt the normal dynamics of endogenous hormones during seed germination, potentially inhibiting germination. In contrast, pre-treating seeds with ABA enhances their ability to cope with environmental stresses, such as drought, salinity, and temperature fluctuations, during germination and early growth stages [7]. For example, ABA priming enhances salt tolerance in maize (*Zea mays*) seedlings by regulating osmotic adjustment, bond energies, reactive oxygen species (ROS) homeostasis, and organic acid metabolism [8]. Seedling survival, plant growth, and grain yield in rice (*Oryza sativa*) were enhanced by ABA priming in saline-alkaline paddy fields [9]. However, while seed priming has shown promise in reducing seed germination time and enhancing seedling survival in adverse soil conditions [10], the germinated seeds still face the challenge of penetrating the crusted soil.

The significance of seedling strength before emergence, particularly in the context of PSCs, underscores the importance of adopting comprehensive assessment parameters [11]. Beyond mere germination time, seedling vigor serves as a critical determinant of successful emergence in challenging soil conditions. The observed correlations between plumule length, diameter, and seedling vigor index highlighted the biomechanical aspects essential for seedlings to penetrate and thrive in PSCs [12, 13]. Longer plumules might suggest stronger seedlings capable of penetrating the soil crust, while thicker plumules indicated greater force to break through soil crusts [14, 15]. Studies on tomato seedlings have also shown that higher mesocotyl and root lengths are directly correlated with enhanced seedling emergence and subsequent growth [16]. The holistic evaluation of seedling vigor, encompassing measurements of plumule and mesocotyl lengths along with seedling dry weight, offers insights into the resilience of seedlings against the formidable challenges posed by PSCs.

Seed germination is a complex and finely orchestrated process governed by a multitude of physiological and biochemical events [17]. During this process, beta-amylase is synthesized de novo, playing a significant role in starch breakdown. Interestingly, the exogenous addition of ABA has been shown to inhibit beta-amylase activity, mRNA accumulation, and the germination process in rice seeds [18]. This highlights the intricate regulatory role of ABA in modulating key enzymes and processes involved in seed germination. As the seed embryo undergoes cellular expansion and elongation, facilitated by the synthesis of new biomolecules, the radicle (embryonic root) emerges to penetrate the seed coat and reach the soil. During this process, primary metabolites such as sugars are broken down from stored reserves like starch, providing the energy required for metabolic processes [19], while amino acids derived from protein breakdown in the seed provide the building blocks for synthesizing new proteins needed for seedling growth [20]. Meanwhile, secondary metabolites, including flavonoids, phenolics, alkaloids, and terpenoids, have been shown serving as defense compounds to protect the seed and emerging seedling from environmental stresses [21]. Flavonoids have antioxidant properties that help scavenge ROS produced during seed germination, protecting the seedling from oxidative damage, and ensuring its survival [22]. Previous studies have indicated that kaempferol, dihydrokaempferol, dihydroquercetin and dihydromyricetin have antioxidant capacity, which can scavenge excessive ROS and mitigate the damage of salt stress on plant cell membranes and enzyme systems [23, 24]. In addition, these flavonoids can regulate the physiological and metabolic processes of plants and enhance the salt tolerance of plants [25]. Studies have shown that ABA is involved in flavonoid biosynthesis [26, 27]. ABA priming may modulate flavonoid biosynthesis during seed germination by reshaping hormone dynamics and altering secondary metabolites, contributing to enhanced seedling resistance to PSCs.

To unravel the mechanisms enhancing the efficacy of ABA seed priming on seedling emergence in PSCs, we conducted comprehensive physiology, metabolome, and transcriptome analyses for germinated seeds and mesocotyls of sweet sorghum. We hypothesized that ABA seed priming might enhance the penetration of sorghum seedlings through the crusted soil by fastening mesocotyl

elongation and strengthening seedling vigor. Our study addressed three main aspects: (1) Investigation of sweet sorghum emergence in saline-alkaline soils; (2) Physiology and metabolome analysis to explore the physio-biochemical mechanisms driving improved seed emergence in PSCs; (3) Transcriptome analysis to elucidate the molecular mechanisms of ABA seed priming. The results of this study provide basic knowledges to obtain optimal sweet sorghum yields in PSCs through ABA seed priming techniques.

Materials and methods

Seed materials, priming treatments and germination experiment

The seeds of *Sorghum bicolor* cv Sb0119, inbred sweet sorghum line, were provided by Sorghum Research Group of Qingdao Agricultural University. The control (CK) group consisted of seeds with no priming. The water treatment (H_2O priming) involved soaking seeds in water, while the ABA treatment used a 20 mg·L^{-1} solution of abscisic acid (ABA). All treatments were conducted under dark conditions at 25 °C for 24 h. After priming, the seeds were rinsed thrice with water to remove excess solution, air-dried until a constant weight was reached. The treatment duration of 24 h and the ABA concentration of 20 mg·L^{-1} were selected based on our previous studies, where these treatments showed significant influence on seed germination [28]. Each batch of 500 g seeds was treated with approximately 2 L of the priming solution. Seed germination was tested in a controlled climate chamber (temperature: 25 °C, humidity: 70.0%, light intensity: 12 K Lux, 14 h light/10 h dark). The primed seeds (CK, ABA-priming, H_2O-priming) were placed on petri dishes (12 × 12 cm) lined with filter paper, ensuring that the paper remained moist. Each priming treatment had four replicates, with 30 seeds per replicate. Seedling morphology, germination rate, and germination speed index were recorded until the completion of germination (7 days).

Pot experiments

All pot experiments were conducted in a greenhouse under controlled conditions (temperature: 25 °C, humidity: 70%, light intensity: 12 K Lux, photoperiod: 14 h of light/10 h of dark), with plants irrigated using tap water. The soil for pot experiment was sampled from a saline-alkaline soil (pH8.50, water soluble salt 3.52 g/kg), air-dried, and passed through a 2 mm mesh sieve to remove stones, plant roots, and leaves. Seeds were sown in plastic pots (13 × 15 × 20 cm), with 30 sorghum seeds per pot.

Pot experiment 1 followed a randomized design with a two-way ANOVA, considering both sowing depth (3 cm, 5 cm, and 7 cm) and treatment type (CK, ABA priming, H_2O priming) as factors. There were three treatment groups and three sowing depths, with each combination replicated four times. Emergence was recorded daily, with data collection concluding on day seven. Seedling penetration through the soil surface was first observed on day four after germination. Emergence rate and germination speed index were calculated for different treatments and sowing depths. Seedlings were extracted from the soil for measurement and photographic documentation of seedling length and root length. At the five-leaf stage, plant height, aboveground biomass and underground biomass were measured.

Pot experiment 2 was a completely randomized design with a one-way ANOVA analysis, focusing on a sowing depth of 5 cm and including six different treatment groups. These treatments included: (1) germinated seeds one day after germination—CKS (control), ABAS (ABA priming), H_2OS (H_2O priming), and (2) mesocotyls from seedlings four days after germination—CKM (control), ABAM (ABA priming), H_2OM (H_2O priming). Each treatment replicated four times. The seeds for one day after germination and mesocotyls four days after germination were collected and quickly cleaned. A portion of the samples was flash-frozen in liquid nitrogen and stored at -80 °C for subsequent analyses, including the contents of phytohormones, carbohydrates, flavonoids, activities of antioxidant enzymes, and the contents of malondialdehyde, proline, and soluble proteins, as well as transcriptome analyses. Another portion of the samples was used to measure mesocotyl length, plumule length, and for cytological observations.

Measurement of germination rate, emergence rate and germination speed index

Seeds were considered germinated when the seminal root reached half of the seed length, and the germination percentage was calculated as the ratio of germinated seeds to total seeds. The emergence rate was determined when the plumule of the germinated seed broke through the physical soil crusts, with the emergence percentage calculated as the ratio of emerged seeds to total seeds. The germination speed index (GSI) was calculated using the formula: $GSI = \Sigma(Gt / Dt)$, where Gt is the number of seeds germinated (or emerged) on day t, Dt is the day of observation (counted from the beginning of the experiment), and t is the day index during the germination or emergence period.

Cytological observation of seedling mesocotyl

Four days after seed germination in soil, the plumule and mesocotyl lengths were measured using vernier caliper. Then, mesocotyl samples were collected for paraffin embedding and thin sectioning. The production protocol followed the method outlined by WC Cornell, et al. [29], but was optimized to meet experimental specifications.

Thin sections were stained with Fast green FCF (OKA Biotechnology Co. LTD., CHINA) and examined under a microscope (Stemi 305, Carl Zeiss AG, Germany) for analysis.

Measurement of phytohormones

The phytohormones were measured according to the method of T Zhao, et al. [30]. Briefly, about 50 mg of seed samples collected 1 day after germination and mesocotyl samples collected on day 4 after germination were combined with an internal standard mixture and an extraction solvent, followed by vortexing and centrifugation. The resulting supernatant is collected, concentrated, and then resuspended before being filtered for analysis using Liquid Chromatography-Electrospray Ionization-Tandem Mass Spectrometry (LC-ESI-MS/MS). The LC mobile phase comprises water with acetic acid (A phase) and acetonitrile with acetic acid (B phase) (Merck Chemical Technology Co., Ltd., Shanghai, China), facilitating the separation of compounds. Gradient elution occurs on a C18 column with specific gradient conditions. Each ion pair is meticulously scanned and detected based on optimized parameters. To quantify hormone levels accurately, concentration standards of hormones like indole-3-acetic acid (IAA), abscisic acid (ABA), and gibberellic acid (GA_3) are employed to establish standard curves (Aladdin Biochemical Technology Co., Ltd., Shanghai, China.). The internal hormone content within the samples is then determined using these standard curves. Data obtained from mass spectrometric detection are subjected to qualitative analysis by integrating peak area ratios and applying linear equations derived from the standard curve.

Measurement of carbohydrates

Carbohydrates were extracted and measured following a modified protocol based on G Ejeta, et al. [31]. The samples used for carbohydrate content analysis were collected simultaneously with those used in the phytohormone assay. Approximately 100 mg of samples were weighed and placed into a 15 mL centrifuge tube, followed by the addition of 2 mL of acetone for extraction. The mixture was shaken at 37 °C for 5 min and centrifuged at 10,000 rpm for 5 min. This step was repeated twice to remove lipids. The precipitate was then treated with 5 mL of preheated 80% ethanol (Aladdin Biochemical Technology Co., Ltd, Shanghai, China.) and shaken for 5 min before heating in a boiling water bath for 30 min with intermittent shaking. After cooling, the sample was centrifuged, and the supernatant was transferred to a 50 mL volumetric flask. This extraction process was repeated thrice. The supernatant was used for reducing sugars and soluble sugars determination, while the precipitate was treated with distilled water and perchloric acid for starch determination. For carbohydrate measurement, 0.2 mL of the extracted solution from each volumetric flask was mixed with anthrone-sulfuric acid solution and heated in a boiling water bath for 10 min. Absorbance was measured at 620 nm. Sucrose determination required the addition of 0.1 mL of 7.6 mol/L KOH before the anthrone-sulfuric acid solution. The content of reducing sugar was calculated by subtracting sucrose content from soluble total sugars. Standard curves using glucose and sucrose solutions (0.0–60.0 μg/mL) were constructed to calculate carbohydrate content in the samples. Each measurement represents the average of four biological replicates ± SD.

Measurement of flavonoids

Flavonoids were analyzed following the protocol outlined by J Meng, et al. [32], with some modifications. About 1 g of germinated seeds and mesocotyls were ground and crushed with liquid nitrogen separately using an MM400 sieve, repeated thrice for consistency. The resulting powder was extracted overnight at 4 °C with 1 mL of 70% methanol (Merck Chemical Technology Co., Ltd., Shanghai, China) containing 0.1 mg L^{-1} lidocaine. After centrifugation and filtration through a 0.22 μm hydrophilic polytetrafluoroethylene syringe filter, the supernatant was prepared for metabolomic analysis. Quality control samples were measured simultaneously with every two experimental samples to ensure repeatability. Metabolites were analyzed using LC-ESI-MS/MS (HPLC, Shim-pack UFLC SHIMADZU CBM30A system; MS, Applied Biosystems 4500Q TRAP). Metabolites were identified and quantified using a comprehensive targeted metabolomic approach provided by MetWare (Wuhan, China), matching accurate m/z values for each precursor ion (Q1) with standards in the self-assembled database. Metabolites exhibiting significant changes were filtered based on $|\text{Log2(Fold change)}| \geq 1$ and p-value < 0.05. Principal component analysis (PCA) of significant changed metabolites was performed using R to explore species-specific accumulation patterns.

Activities of antioxidant enzymes and contents of malondialdehyde, proline and soluble protein

Antioxidant enzyme activities were measured following previous studies, with slight modifications. Briefly, 0.5 g of germinated seeds or mesocotyls were frozen and ground with liquid nitrogen, and the process was repeated three times and passed through an MM400 sieve. Subsequently, the samples were mixed with 0.05 mol/L phosphate buffer (PBS, pH 7.8) (Merck Chemical Technology Co., Ltd., Shanghai, China), thoroughly shaken, and transferred to centrifuge tubes. The mixture was then centrifuged at 4 °C and 12,000 g for 20 min, yielding the enzyme extract in the supernatant. The

activity of superoxide dismutase (SOD) was determined using the p-Nitro-Blue tetrazolium chloride (NBT, Winter song Boye Biotechnology Co., Ltd., Beijing, China) method [33], peroxidase (POD) activity was assessed via the guaiacol (Aladdin Biochemical Technology Co., Ltd., Shanghai, China) method [34]. The activity of catalase (CAT) was assessed by monitoring the degradation of H_2O_2 in a reaction mixture containing 50 mM potassium phosphate buffer (PPB, pH 7.8, Merck Chemical Technology Co., Ltd., Shanghai, China), 10 mM H_2O_2, and 2 mL of enzyme extract. The absorbance of the reaction was subsequently measured at 240 nm [35]. The rate of superoxide anion radical (O_2^-) production was measured through hydroxylamine oxidation (Aladdin Biochemical Technology Co., Ltd., Shanghai, China) [36]. The content of soluble protein (SP) was determined by Coomassie brillant blue (Thermo Fisher Scientific, Waltham, MA, USA) staining [37]. Malondialdehyde (MDA) and proline (Pro) contents were quantified using thiobarbituric acid colorimetric (Thermo Fisher Scientific, Waltham, MA, USA) method [38]. Each treatment was replicated four times for accurate assessment and consistency.

Transcriptome analyses

For the transcriptome analyses, 0.1 g of frozen samples from seeds harvested one day after germination and mesocotyls collected four days after germination were used, with three biological replicates for each treatment. Total RNA extraction was performed for three replications in each treatment using Trizol reagent (Invitrogen, Carlsbad, CA, USA). RNA quality and concentration were assessed using the NanoDrop 2000 spectrophotometer (Thermo Scientific, Wilmington, DE, USA), while RNA integrity was evaluated using the Agent2100 (Agilent Technologies, Santa Clara, CA, USA). Following mRNA extraction, cDNA synthesis, purification, and repair, sequencing through splicing connections was conducted. PCR enrichment was employed to generate cDNA libraries, with Q-PCR ensuring a library concentration exceeding 2nM for quality control. Sequencing was carried out on the Illumina NovaSeq6000 platform, resulting in 119.00 Gb of clean reads with a Q30 base percentage of no less than 94.30% for each sample. HISAT2 [39] software facilitated the rapid and accurate alignment of high-quality clean reads to the reference genome (Sorghum_bicolor.v3.1.1.genome.fa), with StringTie [40] utilized for read assembly and transcriptome reconstruction. Alignment statistics revealed an efficiency of reads mapping to the reference genome ranging between 88.37% and 94.92% for each sample.

In the quantification of gene expression, StringTie was employed, utilizing FPKM (Fragments Per Kilobase of transcript per Million fragments mapped) values greater than 1 as the normalization criterion. Newly identified genes were annotated using DIAMOND [41] and InterProScan [42] software against NR, Swiss-Prot, COG, KOG, KEGG [43] and GO [44] databases. DESeq2 [45] software was employed for comparing differentially expressed genes (DEGs) among CK, ABA priming, and H_2O priming treatments, with Fold Change ≥ 2 and FDR < 0.01 used as filtering criteria during DEGs analysis. ClusterProfiler conducted GO enrichment analysis for biological processes, molecular functions, and cellular components, while KEGG enrichment analysis referenced the KEGG database for significantly enriched pathways of DEGs. Bioinformatics analysis was performed using the pipeline provided by BMKCloud (www.biocloud.net). To validate gene expression levels, qRT-PCR was used on 10 selected DEGs, with β-actin used as internal reference gene (Supplementary Table 1, Supplementary Fig. 1).

Field experiment

The field experiment was conducted in the Agricultural High-tech Industry Demonstration Zone of the Yellow River Delta in Dongying City, Shandong Province (118.65°W, 37.32°N). Characterized by a warm temperate semi-humid monsoon continental climate, the area experiences an annual average temperature of 13.3 °C, annual precipitation of 537 mm, and annual evaporation of 1885 mm. The soil (0–30 cm) was saline-alkaline soil with a pH of 8.5, soil bulk density and electrical conductivity were 1,64 g/cm^3 and 1426.87 us/cm, the contents of soil soluble salts, total organic matter, total nitrogen, total phosphorus and total potassium were 3.52, 5.92, 0.45, 0.16, and 11.43 g/kg, and the contents of available nitrogen, available phosphorus and available potassium were 110.23, 8.17 and 400.32 mg/kg.

Field sowing depths of 3 cm and 5 cm were selected based on the germination results obtained from earlier pot experiments (Fig. 1). The field experiment followed a two-factor design with three priming treatments (CK, ABA priming, H_2O priming) and two sowing depths (3 cm and 5 cm), with plot sizes of 15 m² (3 m × 5 m). Each treatment was replicated three times. Before sowing, 450 kg/hm^2 compound fertilizer (N: P:K = 15:15:15) was applied and incorporated during plowing. The seeds were sown with row space of 40 cm and plant space of 20 cm, covered with soil, and irrigated with water with intensities of 70 mm h^{-1} and 84.10° droplet impact angle according to the references reporting in PSCs [46, 47]. The surface soil was observed for the formation of PSCs, and the seedling emergence rate were recorded 10 days after irrigation. Due to low rainfall in May, the seedlings were rewatered once after seedling establishment 15 days after sowing, then no irrigation was applied. No fertilizer was applied and the plants were weeded manually twice. Before harvest in their maturing stage, plant height and

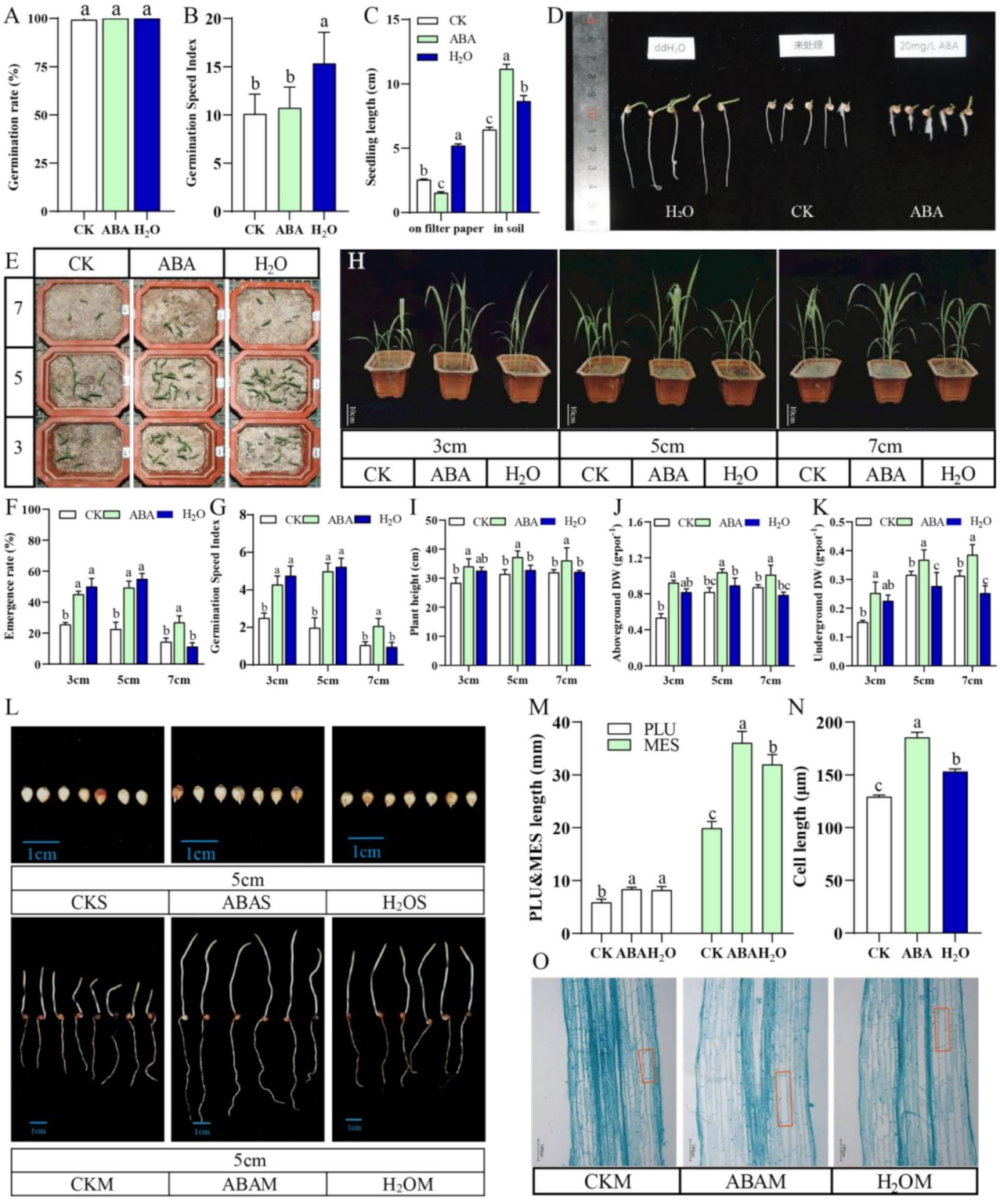

Fig. 1 Effects of ABA priming on the emergence and growth of sorghum seedlings in physical soil crust (PSCs) of saline-alkaline soil. (**A**, **B**, **C**) germination rate, germination speed index, and seedling length of seedlings on filter paper and in soil on day 4 after germination. (**D**) Seedlings germinated on filter paper after 4 day. (**E**) Seedlings at day 7. (**F**) Emergence rate at day 7. (**G**) Germination speed index 1–7 days. (**H**) Phenotype of seedling at five-leaf stage, bar = 10 cm. (**I**) Plant height. (**J**) aboveground biomass and (**K**) underground biomass at five-leaf stage. (**L**) Figures of germinated seeds one day after germination and seedlings four day after germination in PSCs. (**M**) Mesocotyl cells at day four, bar = 100 μm. (**N**) Length of plumule and mesocotyl. (**O**) Length of mesocotyl cell. Data are the means ± standard error ($n = 4$), with different lowercase letters above data bar showing significant differences according to the least significant difference test ($P < 0.05$)

stem diameter were recorded, and the fresh aboveground biomass was measured.

Statistical analyses and data integration

All data plotting and statistical analyses were performed with GraphPad Prism 8.0.2(263) software (https://www.graphpad.com/), and IBM SPSS 26.0 software (https://www.ibm.com/spss). All values are presented as means ± SE. One-way or two-way ANOVA analysis was applied to compare plant height, dry weight, stem diameter, emergence rate, rate of O_2^-, content of MDA, pro, SP, SOD, POD and CAT activities (SPSS 17.0, Chicago, USA). Significance was tested according to the least significant difference test at $P < 0.05$. We used the ClueGO package in Cytoscape software (version 3.9.0) [48, 49] to construct KEGG enrichment analysis network and to perform GO enrichment analysis of functional networks associated with relevant biological processes. The annotation source was *Sorghum bicolor* [taxon ID: 4558], and the kappa score level was set to 0.3. For the comparative analyses, networks of the top 20 significantly enriched KEGG pathways, as well as GO networks in germinating seeds and seedling mesocotyls, were generated. Additionally, we performed a co-expression network analysis in Cytoscape to correlate the 10 differentially expressed genes (DEGs) associated with flavonoid biosynthesis with the differentially expressed metabolites (DEMs) identified. Among them, the DEGs showed significant correlations with key DEMs (|Pearson correlation coefficients| ≥ 0.9).

Results

Seed priming with ABA improved sorghum emergence in saline-alkaline soils

When germinated on filter paper, the germination rates of seeds undergoing priming treatments approached 100%, indicating high seed vigor (Fig. 1A). Compared to the CK, H_2O priming significantly increased the germination speed index, accelerated seed germination, and promoted seedling length, four days after germination. In contrast, ABA priming had no significant effect on the germination speed index under the same conditions but moderately inhibited seedling length (Fig. 1B, C, D).

Pot experiments demonstrated that ABA-primed seeds exhibited higher emergence rates and germination speed index when sown in saline-alkaline soils (Fig. 1E, F, G). Among the three different sowing depths, ABA-primed seeds showed superior seedling emergence morphology compared to H_2O-primed and CK treatments (Supplementary Fig. 2A). ABA priming significantly enhanced seedling length and root length under saline-alkaline soil conditions (Supplementary Fig. 2B, C). Additionally, the ABA-primed seedlings had higher plant height, aboveground biomass and underground biomass when compared with the non-primed ones and those primed with H_2O, particularly at sowing depths of 5 cm and 7 cm (Fig. 1H, I, J, K).

To elucidate the underlying mechanisms by which ABA priming enhanced seedling penetration and growth under saline-alkali soil conditions, detailed observations were made on seeds germinated one day and mesocotyl four days after germination at a sowing depth of 5 cm. ABA priming significantly influenced the morphology of soil-grown seedlings compared to those germinated for four days on filter paper. Specifically, ABA priming led to a 73.58% increase in seedling length relative to the control (Fig. 1L, C). Further morphological analyses revealed that ABA priming markedly promoted the elongation of the plumule and mesocotyl, highlighting its critical role in facilitating seedling development under adverse soil conditions. Specifically, compared to CK, ABA seed priming resulted in a 43.8% and 81.26% increase in the length of the plumule and mesocotyl (Fig. 1M), and led to a significant increase in the length of mesocotyl cells by 43.52% (Fig. 1N). Cell morphology investigations also indicated that the longer mesocotyl length in ABA-primed seedlings was attributed to higher cell length of mesocotyl (Fig. 1O).

Plant hormones involved in ABA seed priming

The dynamic changes in endogenous phytohormones in germinated seeds (one day after germination) and mesocotyls of seedlings (four days after germination) under saline-alkali soil conditions were evaluated. Following ABA priming, significant alterations were observed in the levels of 24 endogenous plant hormones, which orchestrated a wide range of physiological processes crucial for seedling development. Compared to the control and H_2O priming, ABA concentration was the highest in germinated seeds and the lowest in mesocotyls in ABA-primed samples (Fig. 2A). JA levels, including JA-ILE, JA, OPC-4, OPDA, and JA-Val, increased from germinated seeds to mesocotyls but decreased with ABA priming (Fig. 2B). GA concentrations were higher in germinated seeds and rapidly declined in mesocotyls, with ABA priming elevating GA_5 and GA_9 in germinated seeds and GA_{15} in both germinated seeds and mesocotyls (Fig. 2C). Ethylene levels increased significantly by 19.56% in germinated seeds after ABA priming, and by 191.61% and 29.04% in mesocotyls compared to the control and H_2O priming, respectively (Fig. 2D). Auxin and cytokinin levels followed similar patterns to GA, with increases in OxIAA, MEIAA, IAN, and IAA-Ala in germinated seeds, and IAA-Asp and IAA-Glu in both germinated seeds and mesocotyls (Fig. 2E and F).

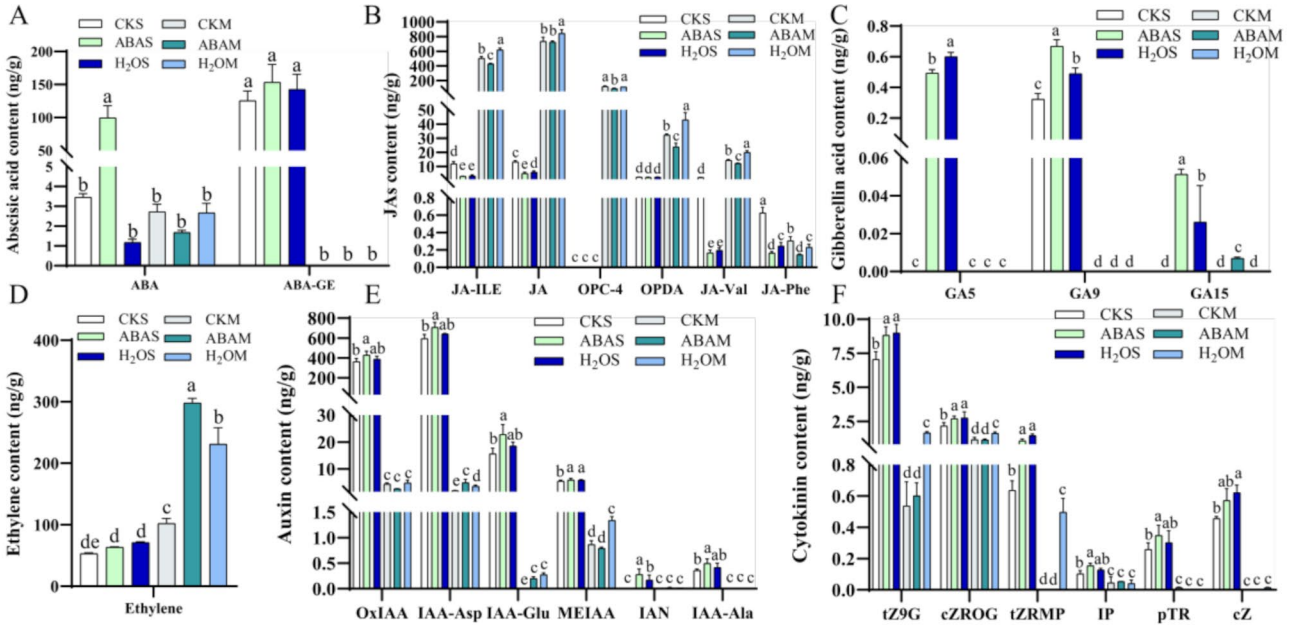

Fig. 2 Endogenous phytohormone contents in the germinated seeds one day after germination and seedling mesocotyls four days after germination under CK, ABA priming and H_2O priming. (**A**) Abscisic acid. (**B**) Jasmonic acid. (**C**) Gibberellin acid. (**D**) Ethylene. (**E**) Auxin. (**F**) Cytokinin. Data are the means ± standard error ($n = 4$), with different lowercase letters above data bar showing significant differences according to the least significant difference test ($p < 0.05$)

Transcriptome analysis during seed germination

Principal component analysis (PCA) revealed a clear separation among samples subjected to different priming treatments, particularly between germinated seeds one day after germination and mesocotyls from seedlings four days after germination. The first two principal components, PCA1 (54.5%) and PCA2 (12.8%), together accounted for 67.3% of the total variance, indicating a dynamic gene expression pattern during sorghum germination (Fig. 3A). Furthermore, PCA displayed a lower variability among biological replicates, suggesting strong correlations between them, which was further supported by samples correlation analysis (Fig. 3A, B). Hierarchical cluster analysis (HCA), based on the relative expression levels of genes associated with germinated seeds and mesocotyls at different developmental stages, demonstrated significant changes in gene expression during seed germination, further confirming the PCA results (Fig. 3C). Comparative analyses between CKS vs. ABAS and H_2OS vs. ABAS revealed 4992 DEGs, with 393 specifically regulated by ABA priming. Similarly, in comparisons between CKM vs. H_2OM and H_2OM vs. ABAM, 1942 DEGs were identified, with 241 specifically regulated by ABA priming (Fig. 3D).

GO and KEGG enrichment analysis of DEGs

The biological functions of the DEGs were comprehensively analyzed through Gene Ontology (GO) and Kyoto Encyclopedia of Genes and Genomes (KEGG) enrichment analyses. The top 10 significantly enriched GO terms (p-value < 0.05) for each cluster across the four comparisons are presented in Supplementary Fig. 3A. Among the four comparisons, eight GO terms were commonly annotated, including the hydrogen peroxide catabolic process, and the apoplast, cell wall, extracellular region, plant-type cell wall and plasmodesma. Additionally, heme binding and peroxidase activity were identified.

The functional networks of biological processes enriched by DEGs in the four comparison groups were further analyzed. DEGs in the CKS vs. ABAS comparison were predominantly associated with various processes, including the abscisic acid-activated signaling pathway, carbohydrate metabolic processes, cell wall biogenesis, lignin biosynthesis process, response to abiotic stimulus, regulation of oxidative stress response, hydrogen peroxide catabolic process, regulation of the jasmonic acid-mediated signaling pathway, systemic acquired resistance, and cell division-related processes such as mitotic cell cycle phase transition, among others (Supplementary Table 2). DEGs identified in the H_2OS vs. ABAS comparison were mainly associated with pathways related to plant hormone regulation (abscisic acid-activated and auxin-activated signaling), morphogenesis, translational elongation, response to oxidative stress, response to salt stress and response to hydrogen peroxide. Notably, no significant enrichment was observed in carbohydrate metabolism (Supplementary Table 3). In

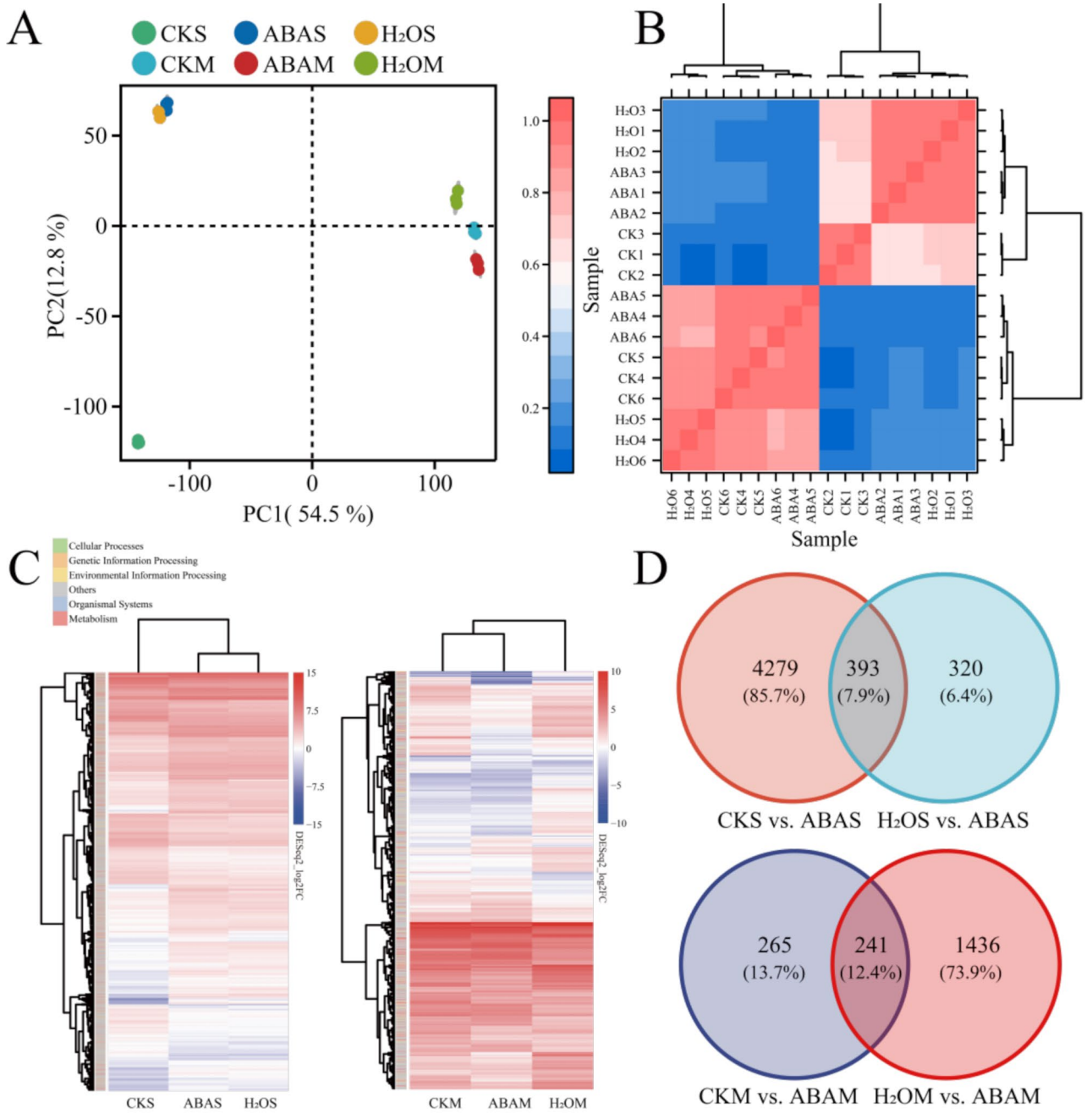

Fig. 3 Transcriptome analysis for germinated seeds and seedling mesocotyls of sweet sorghum at sowing depth of 5 cm in PSCs. (**A**) Principle component analysis (PCA) between treatments ($n=3$). (**B**) Correlation heatmap between samples. X-axis: sample IDs; Y-axis: corresponding sample IDs. Colour indicates R^2 value. (**C**) Hierarchical clustering heatmap of gene expression levels in germinated seeds (left) and seedling mesocotyls (right), calculated as|log2FC|≥1 and FDR < 0.01. (**D**) Venn diagram showing DEG numbers across CKS vs. ABAS and H_2OS vs. ABAS for germinated seeds and CKM vs. ABAM and H_2OM vs. ABAM for seedling mesocotyls

the CKM vs. ABAM comparison, DEGs were predominantly linked to abscisic acid-activated signaling, auxin-activated signaling pathway, carbohydrate metabolism, response to oxidative stress, response to hydrogen peroxide, systemic acquired resistance, and cell wall development processes (Supplementary Table 4). In the H_2OM vs. ABAM comparison, DEGs were primarily associated with responses to salt stress, oxidative stress, ethylene signaling, phototropism, cytokinin regulation, auxin-activated signaling pathway and cell wall development (Supplementary Table 5). Compared to H_2O priming, ABA priming enhanced stress responses and cell development, suggesting a stronger role in overcoming PSCs through

hormonal and signaling pathways, particularly involving ethylene.

Comparative analyses among CKS vs. ABAS, H_2OS vs. ABAS, CKM vs. ABAM, and H_2OM vs. ABAM identified the top 20 KEGG pathways with significant DEG enrichment (Supplementary Fig. 3B). Notably, phenylpropanoid and flavonoid biosynthesis pathways were enriched across all comparisons, underscoring the enhanced role of secondary metabolic pathways in ABA-primed seeds. Additionally, pathways related to starch and sucrose metabolism, plant hormone signal transduction and MAPK signaling were enriched in all comparisons except H_2OS vs. ABAS, suggesting that both ABA and H_2O priming aid germination by mobilizing seed reserves and modulating hormone interactions to support seedling emergence and growth (Supplementary Fig. 3B).

Starch and sucrose metabolism induced by ABA seed priming

Among the DEGs of germinated seeds (393 DEGs) and mesocotyls (241 DEGs) specifically regulated by ABA, a total of 13 DEGs were enriched in the Starch and sucrose metabolism KEGG pathway, including the genes encoding glycogen phosphorylase (PYG), starch synthase (glgA), trehalose-6-phosphate phosphatase (otsB), alpha-amylase (AMY), beta-amylase (BAM), beta-fructofuranosidase (INV) and others (Fig. 4A). The heatmap analysis revealed that the DEGs enriched in this pathway were predominantly upregulated in germinated seeds and mostly non-expressed or downregulated in seedling mesocotyls. To further investigate the relationship between DEGs and the primary altered carbohydrates in seed reserves, this study systematically constructed the KEGG pathways for starch and sucrose metabolism in germinated seeds and seedling mesocotyls (Fig. 4B). Upregulation of genes responsible for hydrolyzing large molecule sugars such as starch and sucrose into small molecule sugars like glucose and fructose was observed, particularly in germinated seeds, involving *AMY*, *BAM*, *INV*, *EG* and *otsB*, etc. Further analyses revealed that ABA priming enhanced soluble total sugar accumulation (Fig. 4C, D, E, F).

ABA seed-priming altered the synthesis of flavonoids

Seven enzymes, encoded by 10 DEGs associated with flavonoid biosynthesis in sorghum, participated in four distinct metabolic pathways of flavonoid biosynthesis pathways. These included genes encoding chalcone synthase (CHS), shikimate O-hydroxycinnamoyltransferase (HCT), bifunctional dihydroflavonol 4-reductase (DFR), naringenin 7-O-methyltransferase (NOMT), 4'-methoxyisoflavone 2'-hydroxylase (CYP81E), isoflavone 7-O-glucoside-6 "-O-malonyltransferase (IF7MAT) and anthidin reductase (ANR) (Fig. 5A). Additionally, 52 differentially expressed metabolites (DEMs) of flavonoid were detected in germinated seeds and mesocotyls, categorized into seven groups (Table 1): anthocyanins (15), Flavones (3), flavonols (7), isoflavones (6), flavanones (7) and Other flavonoids (14). Furthermore, three types of coumarin compounds, including 7-hydroxycoumarin, isofraxindin and scopoletin were enriched in germinated seeds and mesocotyls.

In the subsequent analysis, genetic and metabolic co-expression network were constructed for DEGs and DEMs enriched in flavonoid biosynthesis pathways (Fig. 5B). The accumulation levels of 48 DEMs were regulated by 10 DEGs, with 17 key DEMs showing a significant correlation with these DEGs (|Pearson correlation coefficients| ≥ 0.9). For example, phloretin exhibited a positive correlation with *CHS* and a negative correlation with *CYP81E*. Apigenin showed positive correlations with *CHS*, *NOMT*, and *DFR*. Kaempferide demonstrated a negative correlation only with *HCT*. Dihydrokaempferol was positively correlated with *CHS*, *ANR*, *DFR*, and *NOMT*, while it exhibited both positive and negative correlations with *HCT*. Similar patterns were observed for other DEMs.

To further explore the relationship between DEGs and DEMs involved in flavonoids synthesis, this study systematically constructed the flavonoid biosynthetic pathway during seed germination and seedling development in sorghum (Fig. 6). The pathway included the upstream secondary metabolite pathway: phenylpropanoid biosynthesis KEGG pathway, flavones and flavonol biosynthesis KEGG pathway, isoflavones biosynthesis KEGG pathway and anthocyanins biosynthesis KEGG pathway. Across 18 branches in the flavonoid biosynthesis pathways, 10 DEGs related to flavonoid synthesis and metabolism were annotated (Fig. 5A), and 7 DEGs were observed in the flavonoid biosynthesis KEGG pathway, and 1 DEG was observed in the flavone and flavonol biosynthesis KEGG pathway. Similarly, 2 DEGs in the isoflavonoid biosynthesis KEGG pathway reflected an intricate regulatory network influenced by ABA priming. Notably, DEGs related to flavonoid synthesis exhibited an upregulation trend in germinated seeds. For instance, key enzymes involved in flavonoid biosynthesis pathways, such as *CHS*, *HCT*, *NOMT* and *ANR*, displayed relatively higher expression levels in germinated seeds primed by ABA, benefiting seedling resistance. Conversely, some genes, such as *CYP81E* and *IF7MAT*, demonstrated a downregulation trend in the mesocotyl, indicating tissue-specific regulation of flavonoid metabolism. Concurrently, 17 key DEMs were annotated in the flavonoid biosynthesis pathways and significantly changed in germination seeds and mesocotyls. For example, the contents of liquiritigenin, apigenin and kaempferide in ABA-primed ones were reduced in germinated seeds but increased in mesocotyl.

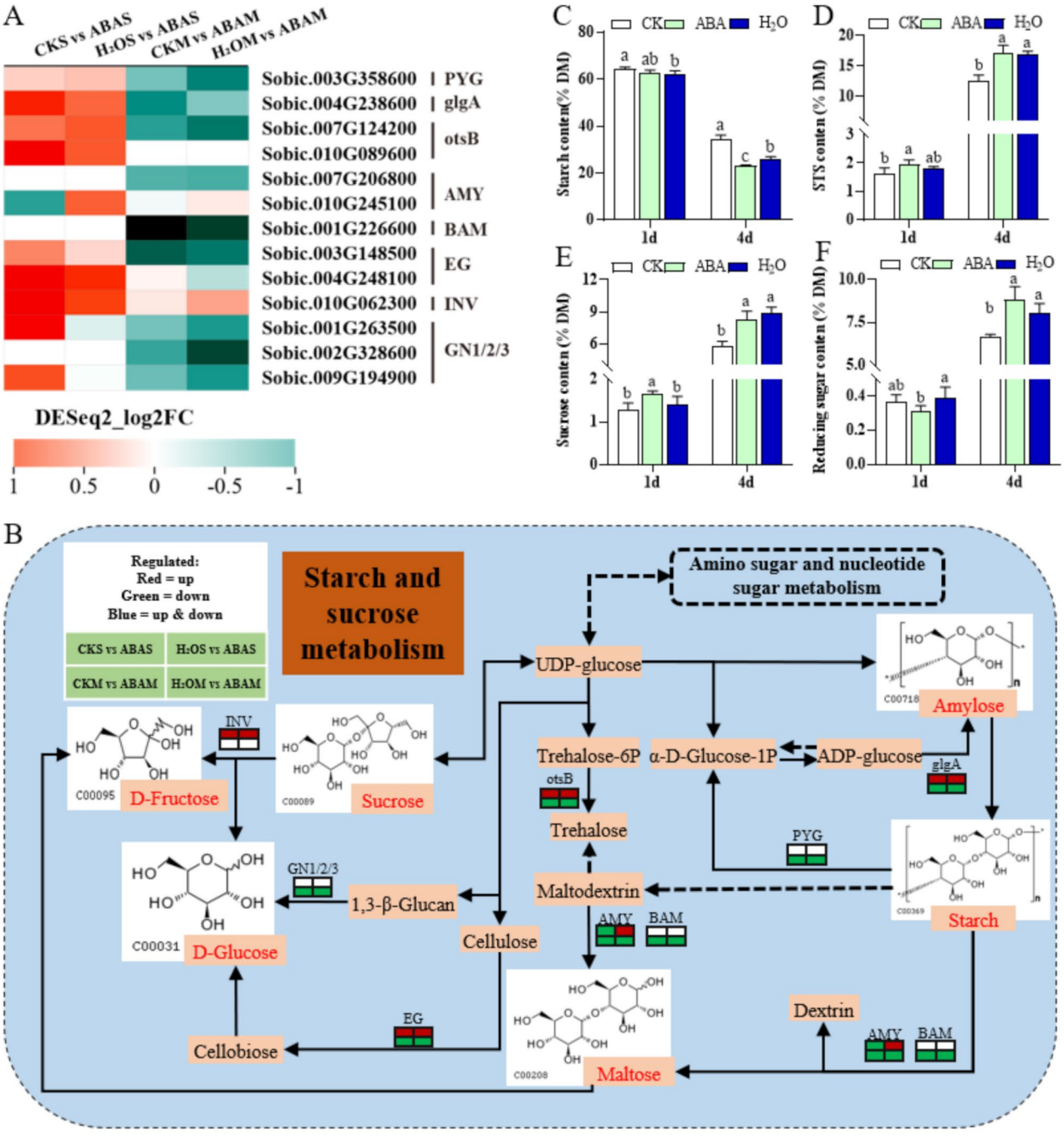

Fig. 4 Influences of ABA priming on starch and sucrose metabolisms of the germinated seeds one day after germination and seedling mesocotyls four days after germination. (**A**) Heat map of DEGs enriched on starch and sucrose biosynthesis KEGG pathway across CKS vs. ABAS and H_2OS vs. ABAS for germinated seeds and CKM vs. ABAM and H_2OM vs. ABAM for seedling mesocotyls. (**B**) Schematic diagram of main starch and sucrose metabolisms KEGG pathways in germination seeds and mesocotyl with ABA priming in physical soil crusts. The brown squares represent carbohydrates involved in the pathway, with the primary altered carbohydrates highlighted in red, while white squares depict their chemical structures. Carbohydrates are linked to their associated differentially expressed genes (DEGs) by arrows, with DEGs represented in color-coded squares: the upper half indicates DEGs in germinated seeds, and the lower half indicates DEGs in the seedling mesocotyls. Squares filled with white represent no DEGs, red indicates upregulation, green indicates downregulation, and blue signifies both upregulation and downregulation. (**C**) Contents of c starch. (**D**) soluble total sugars (STS). (**E**) sucrose and **F** reducing sugar. Data are the means ± standard error ($n = 4$), with different lowercase letters above data bar showing significant differences according to the least significant difference test ($P < 0.05$)

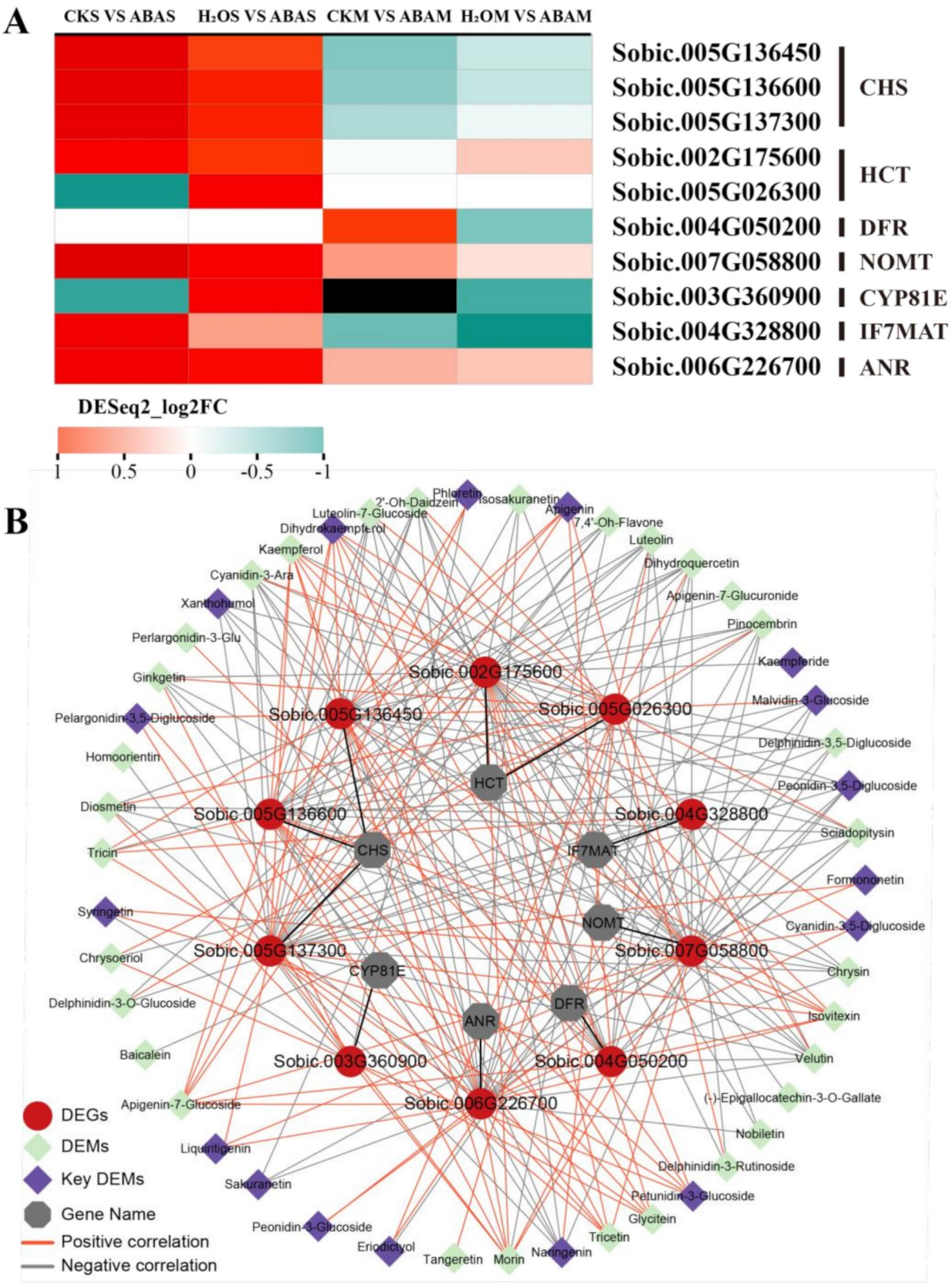

Fig. 5 Co-expression network between the differentially expressed genes (DEGs) and differential expressed metabolites (DEMs) in flavonoid biosynthesis pathway. (**A**) 10 DEGs related to flavonoids biosynthesis KEGG pathway. (**B**) The DEGs and DEMs co-expression network, DEGs was significantly correlated with Key DEMs (|Pearson correlation coefficients| ≥ 0.9, $p < 0.05$)

Table 1 Influences of ABA priming on amounts of flavonoids identified in germinated seeds one day after germination and seedling mesocotyls four day after germination in sweet sorghum. Data are the means ± standard error ($n = 4$), with different lowercase letters after data within each row showing significant differences according to the least significant difference test ($P < 0.05$)

Class	Compounds	Seeds			Mesocotyls		
		CKS	ABAS	H_2OS	CKM	ABAM	H_2OM
Anthocyanins	Cyanidin-3,5-Diglucoside	0e	42.50 ± 5.61b	0e	36.86 ± 1.89c	69.29 ± 6.87a	17.49 ± 3.85d
	Cyanidin-3-Ara	255.49 ± 52.30a	242.37 ± 35.16b	138.34 ± 29.96b	131.35 ± 14.58b	57.22 ± 3.70c	126.77 ± 22.87b
	Delphinidin-3,5-Diglucoside	314.77 ± 4.46b	119.25 ± 20.02d	425.97 ± 45.36a	109.61 ± 20.81e	150.99 ± 16.79c	81.69 ± 9.41f
	Delphinidin-3-O-Glucoside	106.66 ± 6.37a	0b	0b	0b	0b	0b
	Delphinidin-3-Rutinoside	358.76 ± 56.00a	0b	0b	0b	0b	0b
	Malvidin-3,5-Digalcoside	0.57 ± 0.17bc	1.60 ± 0.13a	0.09 ± 0.01d	0.69 ± 0.14b	0.23 ± 0.01 cd	0.31 ± 0.12c
	Malvidin-3-Arabinoside	22.69 ± 4.51a	17.93 ± 4.74b	4.09 ± 0.45d	8.02 ± 2.64c	5.23 ± 0.90 cd	5.99 ± 0.69 cd
	Malvidin-3-Glucoside	0c	10.70 ± 0.75b	0c	0c	22.25 ± 2.06a	0c
	Pelargonidin-3,5-Diglucoside	4.53 ± 0.09c	168.66 ± 5.28bc	203.77 ± 11.07ab	0d	213.19 ± 19.80a	175.04 ± 28.49b
	Peonidin-3,5-Diglucoside	483.32 ± 25.75b	311.64 ± 21.33c	893.18 ± 40.16a	79.81 ± 10.02e	181.56 ± 10.75d	40.37 ± 8.96f
	Peonidin-3-O-Galactoside	0b	0b	0b	0b	36.53 ± 2.48a	0b
	Peonidin-3-Glucoside	415.29 ± 54.83c	654.58 ± 50.80b	302.58 ± 33.97d	294.15 ± 11.45e	276.34 ± 30.60e	715.57 ± 54.30a
	Perlargonidin-3-O-Glucoside	499.05 ± 79.78b	355.24 ± 26.96c	281.62 ± 14.54d	316.01 ± 20.37d	275.58 ± 56.83d	1042.54 ± 84.55a
	Petunidin-3-O-Galactoside	259.14 ± 33.68b	341.91 ± 65.88a	121.04 ± 28.94c	266.70 ± 26.29b	225.12 ± 28.68b	232.96 ± 24.14b
	Petunidin-3-Glucoside	146.62 ± 21.70e	533.67 ± 17.81b	77.74 ± 9.30f	728.04 ± 52.23a	370.44 ± 37.60c	257.90 ± 23.55d
Flavones	Apigenin	0.005 ± 0.00c	0.002 ± 0.00 cd	0.03 ± 0.00a	0.002 ± 0.00 cd	0.02 ± 0.00b	0.004 ± 0.00c
	Chrysoeriol	1.79 ± 0.38a	0.40 ± 0.03c	0.30 ± 0.36c	1.03 ± 0.09b	0.15 ± 0.03d	0.31 ± 0.02c
	Luteolin	0.16 ± 0.01ab	0.17 ± 0.04a	0.09 ± 0.01b	0.006 ± 0.00c	0.009 ± 0.00bc	0.004 ± 0.00 cd
Flavonols	Dihydroquercetin	21.31 ± 1.88a	12.89 ± 1.30b	6.89 ± 0.29c	0.01 ± 0.01d	0d	0.03 ± 0.01d
	Isovitexin	0.13 ± 0.02c	0.01 ± 0.00d	0.03 ± 0.00d	0.26 ± 0.04b	0.14 ± 0.02c	0.36 ± 0.04a
	Kaempferide	0.07 ± 0.03b	0.01 ± 0.02c	0.34 ± 0.07a	0.04 ± 0.01bc	0.06 ± 0.04b	0.07 ± 0.02b
	Kaempferol	0.36 ± 0.02c	0.15 ± 0.01d	0.18 ± 0.07d	4.18 ± 0.43a	3.76 ± 0.35b	3.44 ± 0.30b
	Luteolin-7-O-Glucoside	0.14 ± 0.01a	0.11 ± 0.02b	0.07 ± 0.01c	0.005 ± 0.00e	0.02 ± 0.00d	0.02 ± 0.00d
	Morin	0.05 ± 0.02d	0.06 ± 0.01d	0.06 ± 0.02d	0.46 ± 0.09a	0.27 ± 0.03c	0.34 ± 0.06b
	Syringetin	0.02 ± 0.01 cd	0.03 ± 0.01c	0.05 ± 0.00b	0e	0.01 ± 0.00d	0.09 ± 0.03a
Isoflavones	Phloretin	0c	2.39 ± 0.61b	3.84 ± 0.34a	0c	4.05 ± 0.53a	0c
	2′-Hydroxydaidzein	0.018 ± 0.00a	0.01 ± 0.00b	0.01 ± 0.00b	0.002 ± 0.00c	0.003 ± 0.00c	0.001 ± 0.00c
	Formononetin	0.0007 ± 0.00b	0.0014 ± 0.00ab	0.0004 ± 0.00c	0.0006 ± 0.00bc	0.0015 ± 0.00a	0.0012 ± 0.00ab
	Glycitein	0.04 ± 0.01c	0.03 ± 0.00c	0.02 ± 0.00c	0.57 ± 0.04a	0.01 ± 0.00c	0.13 ± 0.01b
	Prunetin	0.01 ± 0.00c	0.18a	0.17 ± 0.01a	0.03 ± 0.00b	0.21 ± 0.01a	0.01 ± 0.01c
	Velutin	0.78 ± 0.04a	0.29 ± 0.04b	0.22 ± 0.03c	0.12 ± 0.01d	0.20 ± 0.01c	0.05 ± 0.01e
Flavanones	Dihydrokaempferol	7.77 ± 0.45c	54.01 ± 4.12a	16.38 ± 2.81b	0.005 ± 0.00e	0.01 ± 0.01d	0.02 ± 0.00d
	Eriodictyol	5.41 ± 0.52a	0.18 ± 0.01e	0.16 ± 0.01e	4.35 ± 0.18b	2.83 ± 0.25c	1.76 ± 0.07d
	Naringenin	1.73 ± 0.29a	0.81 ± 0.15b	0.52 ± 0.01c	0.35 ± 0.02d	0.11 ± 0.00e	0.44 ± 0.02d
	Liquiritigenin	0.12 ± 0.03b	0.01 ± 0.00c	0.09 ± 0.01bc	0.03 ± 0.00c	0.39 ± 0.07a	0.05 ± 0.01c
	Nobiletin	0.02 ± 0.00b	0.02 ± 0.01b	0.10 ± 0.02a	0.02 ± 0.00b	0.01 ± 0.00c	0.02 ± 0.00b
	Pinocembrin	0.06 ± 0.01a	0.07 ± 0.00a	0.06 ± 0.01a	0.02 ± 0.00b	0.002 ± 0.00c	0.001 ± 0.00c
	Sakuranetin	0.002 ± 0.00c	0.01 ± 0.00b	0.09 ± 0.01a	0.005 ± 0.004c	0d	0d

Table 1 (continued)

Class	Compounds	Seeds			Mesocotyls		
		CKS	ABAS	H_2OS	CKM	ABAM	H_2OM
Other flavonoids	Tangeretin	0.02 ± 0.00a	0.01 ± 0.00b	0.01 ± 0.00b	0.01 ± 0.00b	0.01 ± 0.00b	0.01 ± 0.00b
	Xanthohumol	0.002 ± 0.00f	0.006 ± 0.00e	0.01 ± 0.00d	0.014 ± 0.00c	0.17 ± 0.02a	0.11 ± 0.01b
	Apigenin-7-Glucoside	0.32 ± 0.05d	0.39 ± 0.01 cd	0.33 ± 0.03d	1.32 ± 0.19b	0.57 ± 0.11c	1.79 ± 0.20a
	Apigenin-7-Glucuronide	2.84 ± 0.26b	1.23 ± 0.39c	1.16 ± 0.13c	6.21 ± 0.30a	0.86 ± 0.05c	6.29 ± 0.63a
	(-)-Epigallocatechin-3-O-Gallate	0.008 ± 0.00b	0.005 ± 0.00c	0.02 ± 0.01a	0.007 ± 0.00b	0.008 ± 0.00b	0.003 ± 0.00d
	Ginkgetin	0.35 ± 0.05a	0.24 ± 0.03b	0.32 ± 0.03a	0.31 ± 0.01a	0.19 ± 0.02c	0.16 ± 0.01c
	7,4′-Oh-Flavone	0.01 ± 0.01a	0.01 ± 0.00a	0.01 ± 0.00a	0c	0.004 ± 0.00b	0.01 ± 0.01a
	Chrysin	0.12 ± 0.01b	0.05 ± 0.02c	0.23 ± 0.03a	0.04 ± 0.01c	0.06 ± 0.02c	0.09 ± 0.01b
	Diosmetin	1.62 ± 0.30a	0.35 ± 0.02d	0.75 ± 0.06b	0.91 ± 0.09b	0.14 ± 0.02e	0.52 ± 0.02c
	Homoorientin	0.005 ± 0.00ab	0.005 ± 0.00ab	0.005 ± 0.00ab	0.003 ± 0.00b	0.006 ± 0.00a	0.005 ± 0.00ab
	Sciadopitysin	0.99 ± 0.17a	0.55 ± 0.05b	0.58 ± 0.05b	0.31 ± 0.04c	0.30 ± 0.03c	0.29 ± 0.05c
	Tricetin	0.05 ± 0.01c	0.02 ± 0.01c	0.04 ± 0.02c	0.16 ± 0.01b	0.45 ± 0.08a	0.15 ± 0.03b
	Tricin	0.31 ± 0.09d	0.81 ± 0.05b	1.41 ± 0.09ab	1.62 ± 0.21a	0.58 ± 0.13c	1.62 ± 0.21a
	Isosakuranetin	0.01 ± 0.00c	0.02 ± 0.00b	0.09 ± 0.01a	0.01 ± 0.01c	0.01 ± 0.00c	0.01 ± 0.00c
Coumarins	7-Hydroxycoumarin	0.02 ± 0.00b	0.09 ± 0.01a	0.006 ± 0.00c	0.001 ± 0.00e	0.002 ± 0.00d	0.002 ± 0.00d
	Isofraxindin	0.002 ± 0.00b	0.006 ± 0.00a	0.002 ± 0.00b	0.004 ± 0.00ab	0.003 ± 0.00b	0.002 ± 0.00b
	Scopoletin	0.06 ± 0.01b	0.08 ± 0.01a	0.03 ± 0.00c	0d	0d	0d

In contrast, the levels of eriodictyol and naringenin decreased in both the germinated seeds and mesocotyls, while sakuranetin increased in the germinated seeds but decreased in the mesocotyls. Furthermore, ABA priming led to increased levels of syringetin, phloretin, formononetin, dihydrokaempferol, and xanthohumol in both germinated seeds and mesocotyls.

Precursor synthesis-related genes for Anthocyanin biosynthesis such as *ANR*, were significantly upregulated in germinated seeds and remained unchanged in mesocotyls for ABA-primed ones. Meanwhile, the contents of cyanidin-3,5-diglucoside, malvidin-3-glucoside and pelargonidin-3,5-diglucoside increased in ABA-primed ones, while the contents of petunidin-3-glucoside and petunidin-3-glucoside increased in germinated seeds and decreased in mesocotyls.

Seed priming with ABA improved seedling antioxidative responses in saline-alkaline soils

Next, seedling antioxidative responses were evaluated to investigate their vigor in saline-alkaline soils. Compared to the control, ABA seed priming led to a significant reduction in O_2^- and MDA levels. Specifically, in the mesocotyl, O_2^- and MDA levels decreased by 16.95% and 17.01%, respectively (Fig. 7A, B). The contents of proline and soluble protein (SP) increased substantially post-priming, with ABA priming demonstrating efficacy in mesocotyl. Proline and SP levels surpassed the control by 25.51% and 31.79% (Fig. 7C, D). Compared with the CK, ABA seed priming significantly increased SOD activity by 16.81% and 15.02%, and CAT activity by 51.96% and 62.53%, in germinating seeds and mesocotyls, respectively (Fig. 7E, F). In contrast, POD activity did not show any significant change in germinating seeds but increased significantly by 9.70% in mesocotyls (Fig. 7G). Overall, ABA seed priming proved effective in mitigating oxidative stress during seed germination.

ABA seed priming enhanced the emergence of sweet sorghum seedlings through PSCs and improved their field performance

Physical soil crusts (PSCs) in saline-alkaline soils typically formed rapidly (approximately 2 days) following heavy rainfall or artificial irrigation as moisture evaporates, with the PSC depth reaching approximately 2.5 cm (Fig. 8A, B). These PSCs significantly influenced the emergence of sweet sorghum (Fig. 8C, D, E), while ABA and H_2O priming increased seedling emergence by 96.44% and 73.24% at a sowing depth of 3 cm, and by 33.34% and 27.37% at 5 cm (Fig. 8F). Although there was no significant difference in plant height at maturity between priming and non-priming treatments (Fig. 8G), ABA seed priming resulted in higher fresh weight and stem diameter, particularly at a seeding depth of 5 cm (Fig. 8H, I).

Discussions

ABA seed priming promoted the emergence and improved field performance of sweet sorghum in PSCs

The rapid formation of PSCs, typically within approximately 2 days following irrigation, significantly impeded sweet sorghum emergence. This phenomenon is consistent with previous studies highlighting the adverse effects of soil crusts on seedling emergence [50, 51]. Soil

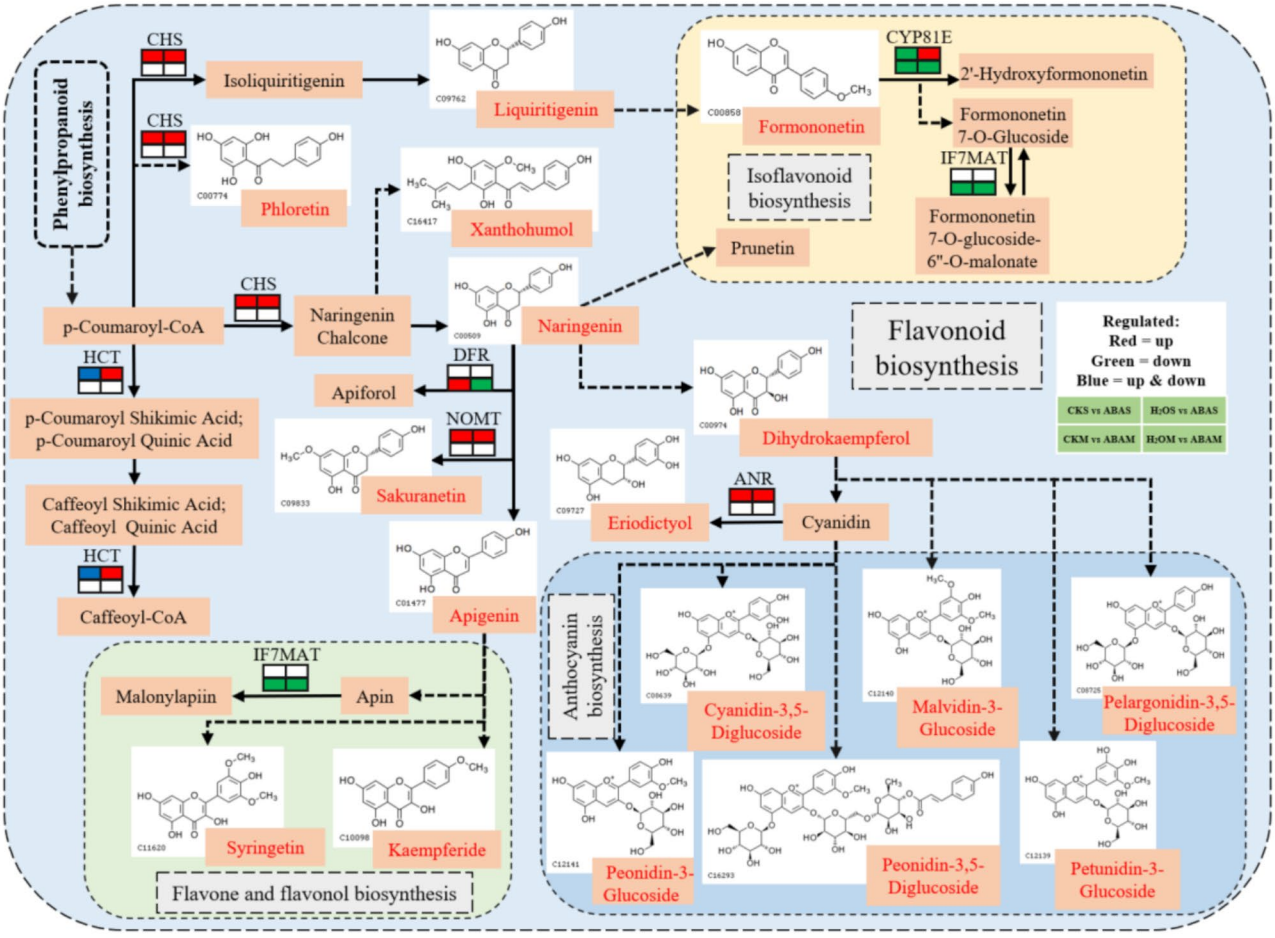

Fig. 6 Schematic diagram of main branches of flavonoid biosynthesis pathways in germinated seeds and seedling mesocotyls by ABA priming in PSCs. Flavonoids changes occur at transcriptome and metabolic levels. The oval box is a partial flavonoid biosynthesis, isoflavonoid biosynthesis, flavone and flavonol biosynthesis, anthocyanin biosynthesis pathway. The brown squares represent the flavonoid compounds involved in the pathway, with the key differentially expressed metabolites (key DEMs) highlighted in red font, while white squares denote their chemical structures. The flavonoid compounds are linked to the differentially expressed genes (DEGs) by arrows, with DEGs represented in color-coded squares: the upper half indicates DEGs in germinated seeds, and the lower half indicates DEGs in the seedling mesocotyls. Squares filled with white represent no DEGs, red indicates upregulation, green indicates downregulation, and blue signifies both upregulation and downregulation

crusts create a hardened surface layer that restricts seedling emergence by impeding seedling penetration and gas exchange, thus hampering root growth and nutrient uptake [51]. ABA seed priming demonstrated clear advantages in enhancing seedling emergence rates, particularly at seeding depths of 5 cm, where emergence rates increased by approximately 33% compared to non-primed seeds. Similar findings have been reported in other crops, where ABA seed priming enhances seedling emergence under various environmental stresses, including salinity and drought [52]. Higher mesocotyl length and plumule length were also observed in ABA-primed seedlings, which might be the main reason contributing to enhanced seedling emergence. Cell morphology investigation in this study indicated that the higher mesocotyl length in ABA-primed seedlings was attributed to higher cell length of mesocotyl. The priming process enables seeds to undergo pre-germination metabolic activation, leading to quicker and more uniform germination, which is crucial for overcoming soil crust impediments [53].

While there were no significant differences in plant height at maturity between primed and non-primed treatments, ABA seed priming led to higher fresh weight and stem diameter, indicating improved early seedling vigor contributing to later improved growth under soil crust conditions. These results align with studies in maize and wheat demonstrating the positive effects of ABA priming on seedling vigor and early growth parameters [8, 54]. The enhanced early growth vigor may be attributed to the improved nutrient mobilization and metabolic processes initiated by ABA priming, allowing seedlings to establish more robust root systems and allocate resources efficiently [55]. By enhancing seedling emergence rates and promoting early growth vigor, ABA

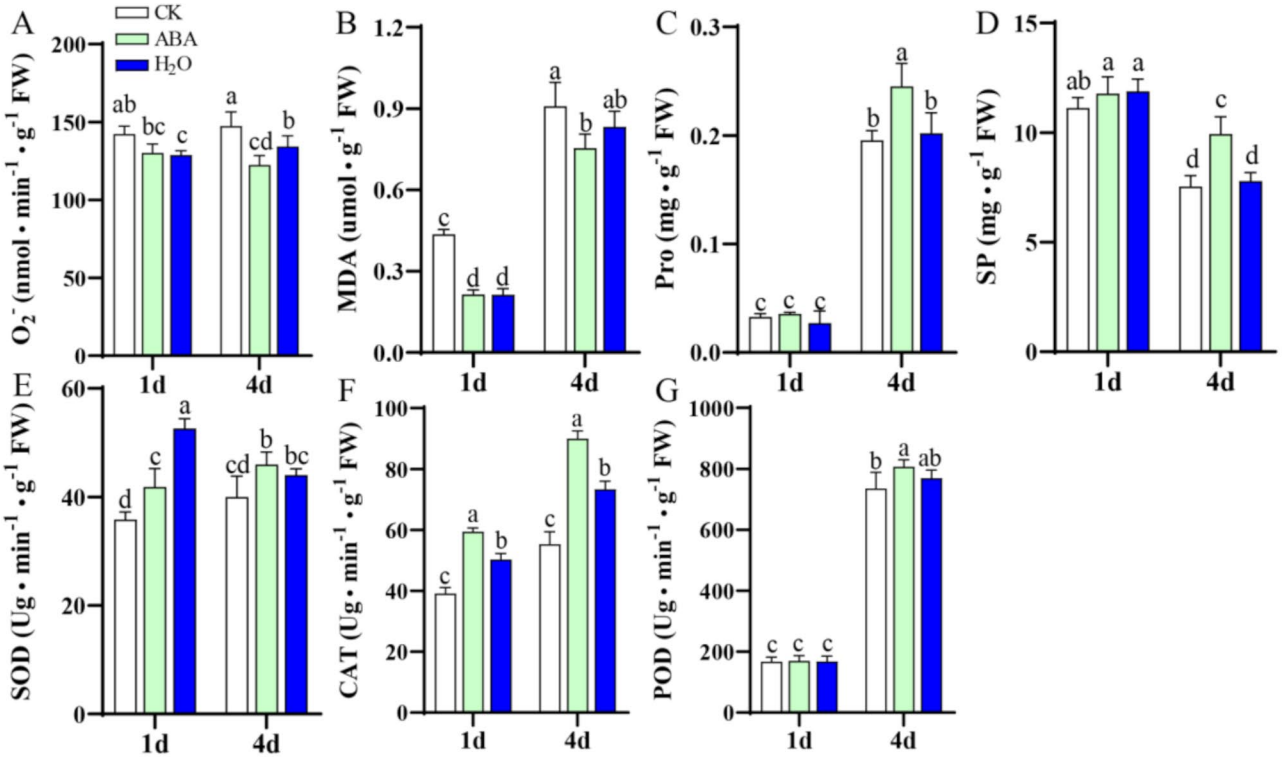

Fig. 7 Influences of ABA priming on antioxidant capacity of the germinated seeds one day after germination and seedling mesocotyls four days after germination. (**A**) Rate of superoxide anion radical (O_2^-) production. (**B**, **C**, **D**) Content of malondialdehyde, proline (Pro) and soluble protein (SP). (**E**, **F**, **G**) Activity of superoxide dismutase (SOD), Catalase (CAT), Peroxidase (POD). Data are the means ± standard error ($n = 4$), with different lowercase letters above data bar showing significant differences according to the least significant difference test ($P < 0.05$)

priming offers a practical strategy to mitigate the challenges posed by PSCs in saline-alkaline soils.

ABA priming reshaped hormonal dynamics in germinating seedlings

ABA seed priming significantly influenced hormone dynamics during seed germination by altering endogenous hormone synthesis pathways [56]. Our investigation revealed notable changes in key plant hormones, demonstrating ABA's role in coordinating hormonal dynamics essential for seedling development and stress response mechanisms. Exogenous ABA application increased endogenous ABA content, impacting seed dormancy release and stress adaptation [57]. In our study, JA levels significantly increased during seed germination, suggesting that JA primarily functions in response to stress. Variations in JA content among different priming treatments were also observed, particularly in relation to the inhibition of mesocotyl elongation [58]. ABA priming influenced GA biosynthesis in the diterpenoid biosynthesis pathway, which is crucial for seed germination and shoot elongation [59].

Additionally, our results indicated a crosstalk between ABA and auxin signaling pathways, coordinating physiological processes vital for seedling establishment. Auxin regulates cell expansion that drives mesocotyl elongation [60], with increasing auxin concentrations correlating with enhanced mesocotyl length. The interaction between ABA and cytokinin biosynthesis and signaling further highlights the complex hormonal interactions that control seed germination and early seedling growth. These findings underscore the regulatory function of ABA seed priming in modulating hormonal dynamics, enhancing seedling vigor, stress tolerance, and overall crop performance in PSCs. Furthermore, ABA regulated the expression of genes related to sugar metabolism, influencing energy release during germination, while also promoting secondary metabolism by regulating the expression of flavonoid biosynthesis genes.

ABA priming fastened starch and sucrose metabolism

Starch and sucrose metabolism play pivotal roles in seed germination by providing energy and essential components for growth [61]. In ABA-primed seedlings, 13 DEGs associated with starch and sucrose metabolism pathways were identified, including those encoding key enzymes such as *AMY*, *BAM* and *INV*, facilitating the breakdown of complex sugars into usable forms [62]. Notably, these genes show upregulation during the early stages of germination, emphasizing their importance in

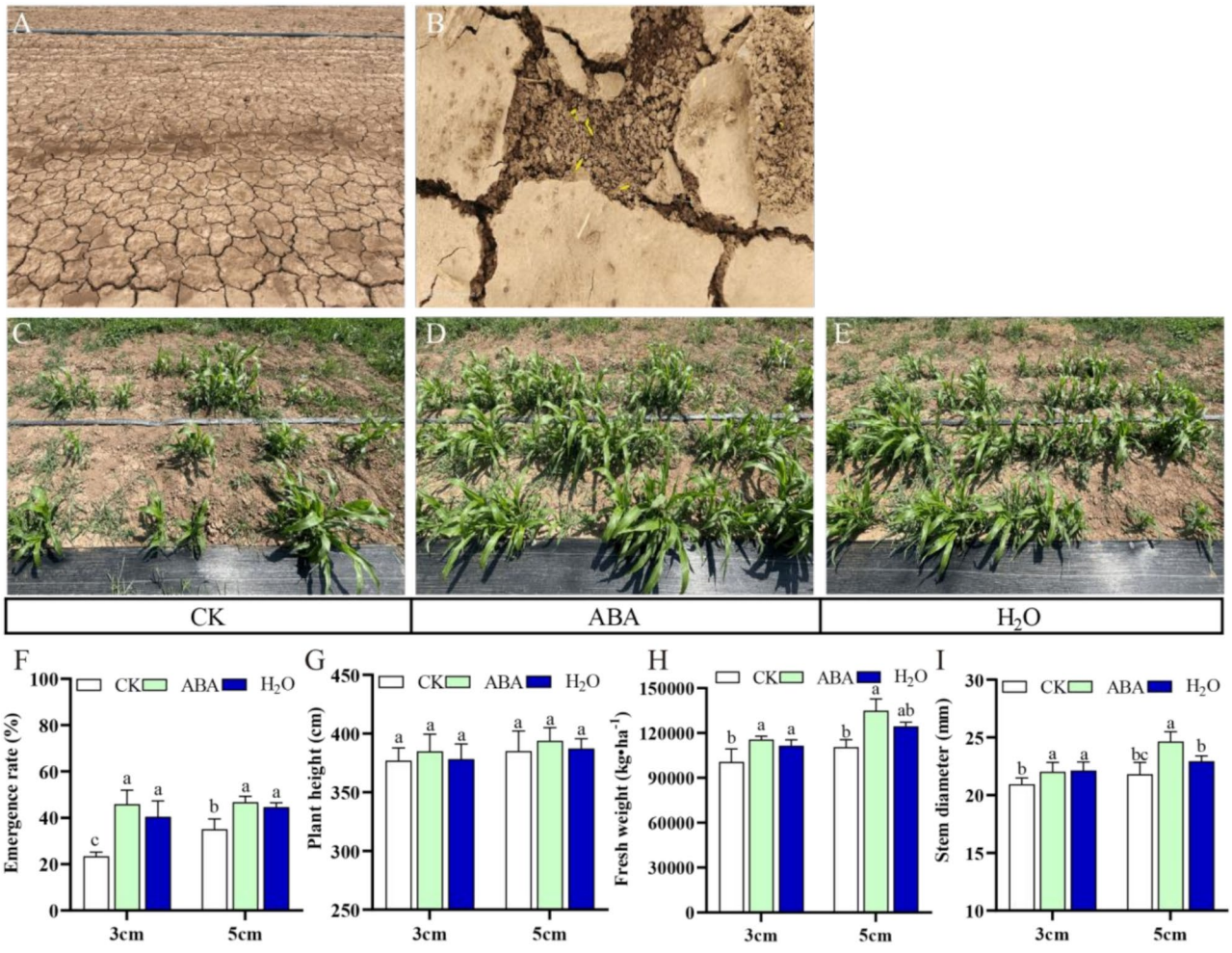

Fig. 8 Influences of ABA priming on seedling emergence and growth of sweet sorghum in physical soil crusts (PSCs). (**A**) Formation of PSCs two days after irrigation. (**B**) Seedlings buried under PSCs. (**C**) Seedling emergence of CK. (**D**) Seedling emergence of ABA-primed seeds. (**E**) Seedling emergence of H_2O-primed seeds. (**F**) Emergence rate. (**G**) Plant height. (**H**) Fresh weight at maturity. (**I**) Stem diameter. Data are the means ± standard error ($n = 3$), with different lowercase letters above data bar showing significant differences according to the least significat difference test ($P < 0.05$)

energy release [63]. Conversely, genes involved in sugar synthesis pathways, like *glgA*, exhibit downregulation, indicating a shift towards sugar catabolism [64]. This dynamic regulation reflects the temporal coordination of starch and sucrose metabolism pathways to meet the metabolic demands during seedling growth [65]. Further analyses revealed that ABA priming enhanced soluble sugar accumulation, indicating increased sucrose metabolism enzyme activity and accelerated starch hydrolysis [66]. This metabolic reprogramming provided the necessary energy reserves to support seed germination and early seedling growth, contributing to enhanced vigor and stress tolerance in PSCs [67].

ABA priming-induced flavonoid modulation enhances seedling resistance to PSCs

ABA seed priming exerted a profound influence on secondary metabolism, particularly in flavonoid biosynthesis, which serves as a cornerstone for stress responses and developmental processes [68]. Across 18 branches in the flavonoid biosynthesis pathways, 10 DEGs related to flavonoid synthesis and metabolism were identified, reflecting an intricate regulatory network influenced by ABA priming. Notably, DEGs related to flavonoid synthesis exhibited an upregulation trend in germinated seeds, suggesting enhanced flavonoid production as a response to ABA priming [69]. For instance, key enzymes involved in flavonoid biosynthesis pathways, such as *CHS*, *HCT*, *NOMT and ANR*, displayed relatively higher expression levels in germinated seeds primed by ABA, benefiting seedling resistance. Modulating the expression levels of *EaCHS1* in tobacco leads to alterations in flavonoid accumulation and plays a regulatory role in enhancing plantlet tolerance to salinity stress by preserving ROS homeostasis [70]. Conversely, some genes, like *CYP81E* and *IF7MAT*, showed

a downregulation trend in the mesocotyl, indicating tissue-specific regulation of flavonoid metabolism. Previous studies have shown that after hormone treatment, the expression of *IF7MaT* in soybean leaves is increased compared with the control, which promotes the synthesis of isoflavones [71]. Therefore, ABA priming differentially influenced the expressions of genes involved in flavonoid biosynthesis, benefiting sweet sorghum seedling emergence in PSCs.

The observed fluctuations in the levels of various flavonoid compounds further underscore the complexity of plant responses to ABA priming and environmental stresses. Flavonoids such as liquiritigenin, apigenin, kaempferide, eriodictyol, naringenin, syringetin, phloretin, formononetin, dihydrokaempferol, and xanthohumol exhibited differential accumulation patterns in germinated seeds and mesocotyls following ABA priming. These fluctuations in flavonoid content may reflect specific metabolic adjustments aimed at enhancing stress resilience, modulating signal transduction pathways, and maintaining cellular homeostasis in response to environmental challenges. For example, the contents of liquiritigenin, known for its antioxidant properties, were significantly higher in alfalfa seedlings of MsMYB741-OE lines than wide type under 7 days' aluminum stress, contributing to alfalfa resistance to aluminum stress [72]. Formononetin might modulate plant-microbe interactions, enhancing plant resilience to pathogens [73], Previous studies have demonstrated that kaempferol and dihydrokaempferol possess antioxidant properties, enabling them to scavenge excessive reactive oxygen species and thereby mitigate the damage caused by salt stress on plant cell membranes and enzyme systems [23, 24]. Additionally, dihydrokaempferol have been shown to accumulate significantly in mulberry (*Morus atropurpurea*) seeds under salt stress, promoting seed germination [74]. An increase of xanthohumol content was observed in salt-stressed *Zygosaccharomyces rouxii*, benefiting its resistance [75]. Apigenin pretreatment was associated with the induction of the rice antioxidant defense system represented by the induced activities of the antioxidant enzymes in the roots [76].

The significant enhancement in antioxidative responses following ABA seed priming suggests its potential as a valuable agronomic practice for improving sweet sorghum emergence and vigor in saline-alkaline soils. Reduced levels of O_2^- and MDA after ABA priming indicate effective oxidative stress alleviation, which is crucial for seedling survival under adverse conditions [77]. The increased proline and SP contents observed, particularly in the mesocotyl, highlights their role in osmotic adjustment and stress resilience, corroborating findings from previous studies that demonstrate their protective functions in stress environments [78]. Our study demonstrates that ABA priming significantly enhanced the activities of SOD, POD and CAT in germinating seeds and the mesocotyl of sorghum, highlighting the critical role of seed priming in mitigating salinity-alkalinity stress. This aligns with the findings of Guo et al. [79], who observed that seed priming with various agents reduced MDA content, enhanced the activities of CAT, POD, and SOD, and increased proline content, thereby alleviating the adverse effects of salt stress on sorghum growth. Furthermore, the elevated activities of antioxidant enzymes such as SOD, POD and CAT following ABA priming align with the known mechanisms where these enzymes mitigate ROS and protect cellular integrity [80]. Such physiological changes might be attributed to the alterations of flavonoids induced by ABA priming. Flavonoids are involved in salt tolerance through ROS scavenging in the halophyte *Atriplex canescens* [81]. *EbbHLH80-OE* plants displayed higher salt tolerance than wild-type plants during seed germination and seedling growth by up-regulating flavonoid accumulation, enhanced levels of antioxidant enzyme expression and Modulating ROS Levels in tobacco [82]. This comprehensive antioxidative response underscores ABA priming's effectiveness in enhancing sweet sorghum's tolerance to the combined stresses of saline-alkaline soils and PSCs, making it a promising technique for improving crop performance under such conditions.

Conclusions

This study highlights the effectiveness of ABA seed priming in enhancing sweet sorghum emergence in saline-alkaline soils, especially in overcoming rapid physical soil crust (PSC) formation. ABA priming improved seedling emergence, early growth, and stress tolerance by activating pre-germination metabolic pathways. Changes in endogenous hormone levels demonstrated ABA's role in coordinating phytohormone dynamics during germination. Transcriptome analysis revealed that ABA priming reprogrammed both primary and secondary metabolic pathways, particularly starch and sucrose metabolism, by upregulating key genes like AMY, BAM, and INV. This facilitated energy mobilization for faster seedling emergence. Additionally, ABA priming induced flavonoid biosynthesis genes (CHS, HCT, DFR, NOMT, and ANR), leading to the accumulation of key flavonoids such as liquiritigenin, apigenin, dihydrokaempferol, and phloretin. These metabolites enhanced antioxidant defense, reduced oxidative damage (O_2^- and MDA), and improved seedling survival under stress. Therefore, ABA priming effectively promotes sweet sorghum seedling emergence in PSCs by accelerating growth, enhancing energy mobilization, and improving stress resistance, thereby supporting better crop establishment under challenging conditions.

Abbreviations

ABA	Abscisic acid
AMY	Alpha-amylase
BAM	Beta-amylase
CAT	Catalase
DEGs	Differentially expressed genes
DEMs	Differentially expressed metabolites
FPKM	Fragments Per Kilobase of transcript per Million fragments mapped
GA	Gibberellic acid
glgA	Starch synthase
IAA	Indole-3-acetic acid
INV	Beta-fructofuranosidase
JA	Jasmonic acid
LC-ESI-MS/MS	Liquid Chromatography-Electrospray Ionization-Tandem Mass Spectrometry
MDA	Malondialdehyde
NBT	P-Nitro-Blue tetrazolium chloride
O_2^-	Superoxide anion radical
otsB	Trehalose-6-phosphate phosphatase
PBS	Phosphate buffer
PCA	Principal component analysis
PLS-DA	Partial least-squares discriminant analysis
POD	Peroxidase
PSCs	Physical soil crusts
PYG	Glycogen phosphorylase
ROS	Reactive oxygen species
SOD	Superoxide dismutase
SP	Soluble protein

Supplementary Information

The online version contains supplementary material available at https://doi.org/10.1186/s12864-025-11420-4.

Supplementary Figure 1: Relative expression of 10 genes involved in germinated seeds as influenced by ABA priming. CHS, Sobic.005G136450.v3.2; ANR, Sobic.006G226800.v3.2; CYP98A, Sobic.003G327800.v3.2; NOMT, Sobic.007G058800.v3.2;HCT, Sobic.003G082900.v3.2; AMY, Sobic.002G225600.v3.2; BAM, Sobic.001G293800.v3.2; SPS, Sobic.003G403300.v3.2; glgA, Sobic.004G238600.v3.2; WAXY, Sobic.010G022600.v3.2. * The Student's t-test was utilized to compare the relative expression levels between the CK (control) and ABA-primed groups. **Supplementary Figure 2**. The germination morphology of sorghum seedlings with CK, ABA, and H_2O priming treatments was observed on day 7 after emergence. A Seedling emergence morphology in soil at sowing depths of 3, 5, and 7 cm under the three priming treatments on day 7 after emergence. B Seedling length in soil. C Root length of seedlings in soil. Data are the means ± standard error ($n = 4$), with different lowercase letters above data bar showing significant differences according to the least significat difference test ($P < 0.05$). **Supplementary Figure 3**. GO and KEGG Enrichment Analysis of Differentially Expressed Genes (DEGs). **A** DEGs enriched on the top 10 GO terms (P value < 0.05) for each of three main GO categories (Molecular Function, Cellular Component and Biological Process) in CKS vs. ABAS, CKS vs. H_2OS, CKM vs. ABAM, and CKM vs. H_2OM. **B** DEGs enriched on the top 20 KEGG pathways in CKS vs. ABAS, CKS vs. H_2OS, CKM vs. ABAM, and CKM vs. H_2OM

Supplementary Table 1: The primers used for qRT-PCR analysis. **Supplementary Table 2**: CKS vs. ABAS_Biological_Process. **Supplementary Table 3**: H_2OS vs. ABAS_Biological_Process. **Supplementary Table 4**: CKM vs. ABAM_Biological_Process. **Supplementary Table 5**: H_2OM vs. ABAM_Biological_Process

Acknowledgements
Not applicable.

Author contributions
JY and WZ carried out the experiments and data analysis. TW, JX, JW, JH, and YS. JY, YN and YG interpreted the results and wrote the manuscript. All authors provided critical feedback, helped shape the research and authorized the final manuscript.

Funding
This study is financially supported by National Key R&D Program of China (2023YFE1304303).

Data availability
The data and supporting sample-specific information discussed in this publication is available on National Center for Biotechnology Information (NCBI) dataset accession number (PRJNA1163929). We confirm that all materials and experiments in this publication were in accordance with the relevant guidelines and regulations.

Declarations

Ethics approval and consent to participate
Not applicable.

Consent for publication
Not applicable.

Competing interests
The authors declare no competing interests.

Author details
[1]College of Grassland Science, Qingdao Agricultural University, Qingdao 266109, China
[2]Qingdao key laboratory of specialty plant germplasm innovation and utilization in saline soils of coastal beach, Qingdao Agricultural University, Qingdao 266109, China
[3]Key Laboratory of National Forestry and Grassland Administration on Grassland Resources and Ecology in the Yellow River Delta, Qingdao Agricultural University, Qingdao 266109, China
[4]College of Agronomy, Qingdao Agricultural University, Qingdao 266109, China

Received: 16 September 2024 / Accepted: 28 February 2025
Published online: 12 March 2025

References

1. Shi X, Xiong J, Yang X, Siddique KHM, Du T. Carbon footprint analysis of sweet sorghum-based bioethanol production in the potential saline-Alkali land of Northwest China. J Clean Prod. 2022;349:131476.
2. Yang R, Sun Z, Liu X, Long X, Gao L, Shen Y. Biomass composite with exogenous organic acid addition supports the growth of sweet sorghum (*Sorghum bicolor*'Dochna') by reducing salinity and increasing nutrient levels in coastal saline-alkaline soil. Front Plant Sci. 2023;14:1163195.
3. Ibrahim MEH, Ali AYA, Elsiddig AMI, Zhou G, Nimir NEA, Ahmad I, Suliman MSE, Elradi SBM, Salih EGI. Biochar improved sorghum germination and seedling growth under salinity stress. Agron J. 2020;112(2):911–20.
4. Assouline S, Thompson SE, Chen L, Svoray T, Sela S, Katul GG. The dual role of soil crusts in desertification. J Geophys Research-Biogeosciences. 2015;120(10):2108–19.
5. Marusig D, Tombesi S. Abscisic acid mediates drought and salt stress responses in *Vitis vinifera*—A review. Int J Mol Sci. 2020;21(22):8648.
6. Sano N, Marion-Poll A. ABA metabolism and homeostasis in seed dormancy and germination. Int J Mol Sci. 2021;22(10):5069.
7. Srivastava AK, Kumar JS, Suprasanna P. Seed 'primeomics': plants memorize their germination under stress. Biol Rev. 2021;96(5):1723–43.
8. Sarkar B, Bandyopadhyay P, Das A, Pal S, Hasanuzzaman M, Adak MK. Abscisic acid priming confers salt tolerance in maize seedlings by modulating osmotic adjustment, bond energies, ROS homeostasis, and organic acid metabolism. Plant Physiol Biochem. 2023;202:107980.
9. Wei LX, Lv BS, Li XW, Wang MM, Ma HY, Yang HY, Yang RF, Piao ZZ, Wang ZH, Lou JH, et al. Priming of rice (*Oryza sativa* L.) seedlings with abscisic acid enhances seedling survival, plant growth, and grain yield in saline-alkaline paddy fields. Field Crops Res. 2017;203:86–93.

10. Khan M, Irfan M, Muhammad A, Ullah I, Ali M, Nawaz S, Khalil M, Manzoor Ahmad D. A practical and economical strategy to mitigate salinity stress through seed priming. Front Environ Sci. 2022;10:991977.
11. Awadhwal NK, Thierstein GE. Soil crust and its impact on crop establishment: A review. Soil Tillage Res. 1985;5(3):289–302.
12. Alom R, Hasan MA, Islam MR, Wang Q. Germination characters and early seedling growth of wheat (*Triticum aestivum* L.) genotypes under salt stress conditions. J Crop Sci Biotechnol. 2016;19(5):383–92.
13. Farsaraei S, Mehdizadeh L, Moghaddam M. Seed priming with Putrescine alleviated salinity stress during germination and seedling growth of *Medicinal pumpkin*. J Soil Sci Plant Nutr. 2021;21(3):1782–92.
14. Khodarahmpour Z. Effect of salinity stress on germination indices of corn (*Zea mays* L.) hybrids. Res Crops. 2012;13(3):846–51.
15. Noorhosseini SA, Jokar NK, Damalas CA. Improving seed germination and early growth of garden Cress (*Lepidium sativum*) and Basil (*Ocimum Basilicum*) with hydro-priming. J Plant Growth Regul. 2018;37(1):323–34.
16. Nakaune M, Tsukazawa K, Uga H, Asamizu E, Imanishi S, Matsukura C, Ezura H. Low sodium chloride priming increases seedling Vigor and stress tolerance to *Ralstonia solanacearum* in tomato. Plant Biotechnol. 2012;29(1):9–18.
17. Paparella S, Araújo SS, Rossi G, Wijayasinghe M, Carbonera D, Balestrazzi A. Seed priming: state of the Art and new perspectives. Plant Cell Rep. 2015;34(8):1281–93.
18. Wang SM, Lue WL, Eimert K, Chen J. Phytohormone-regulated beta-amylase gene expression in rice. Plant Mol Biol. 1996;31(5):975–82.
19. Sami F, Yusuf M, Faizan M, Faraz A, Hayat S. Role of sugars under abiotic stress. Plant Physiol Biochem. 2016;109:54–61.
20. Yang P, Li X, Wang X, Chen H, Chen F, Shen S. Proteomic analysis of rice (*Oryza sativa*) seeds during germination. Proteomics. 2007;7(18):3358–68.
21. Pająk P, Socha R, Gałkowska D, Rożnowski J, Fortuna T. Phenolic profile and antioxidant activity in selected seeds and sprouts. Food Chem. 2014;143:300–6.
22. Flores PC, Yoon JS, Kim DY, Seo YW. Effect of chilling acclimation on germination and seedlings response to cold in different seed coat colored wheat (*Triticum aestivum* L). BMC Plant Biol. 2021;21(1):252.
23. Jan R, Khan M, Asaf S, Lubna, Asif S, Kim K-M. Bioactivity and therapeutic potential of Kaempferol and Quercetin: new insights for plant and human health. Plants. 2022;11(19):2623.
24. Liu D, Mao Y, Ding L, Zeng X-A. Dihydromyricetin: A review on identification and quantification methods, biological activities, chemical stability, metabolism and approaches to enhance its bioavailability. Trends Food Sci Technol. 2019;91:586–97.
25. Agati G, Azzarello E, Pollastri S, Tattini M. Flavonoids as antioxidants in plants: location and functional significance. Plant Sci. 2012;196:67–76.
26. Han C, Chen G, Zheng D, Feng N. Transcriptomic and metabolomic analyses reveal that ABA increases the salt tolerance of rice significantly correlated with jasmonic acid biosynthesis and flavonoid biosynthesis. Sci Rep. 2023;13(1):20365.
27. Wu P, Liu AL, Li LJ. Metabolomics and transcriptome analysis of the biosynthesis mechanism of flavonoids in the seeds of *Euryale ferox* Salisb at different developmental stages. Mol Genet Genomics. 2021;296(4):953–70.
28. Yao L, Qi C, Yang J, Guo Y. Effects of seed priming on cuticular wax and resistance of sweet sorghum. Acta Prataculturae Sinica. 2022;31(7):185–96.
29. Cornell WC, Morgan CJ, Koyama L, Sakhtah H, Mansfield JH, Dietrich LEP. Paraffin embedding and thin sectioning of microbial colony biofilms for microscopic analysis. In: J Visualized Experiments: JoVE. 2018.
30. Zhao T, Deng X, Xiao Q, Han Y, Zhu S, Chen J. IAA priming improves the germination and seedling growth in cotton (Gossypium hirsutum L.) via regulating the endogenous phytohormones and enhancing the sucrose metabolism. Ind Crops Prod. 2020;155:112788.
31. Ejeta G, Axtell JD. Dry-matter accumulation and carbohydrate composition in developing normal- and high-lysine sorghum grain. J Agric Food Chem. 1987;35(6):981–5.
32. Meng J, Wang B, He G, Wang Y, Tang X, Wang S, Ma Y, Fu C, Chai G, Zhou G. Metabolomics integrated with transcriptomics reveals Redirection of the phenylpropanoids metabolic flux in *Ginkgo biloba*. J Agric Food Chem. 2019;67(11):3284–91.
33. Durak I, Yurtarslanl Z, Canbolat O, Akyol O. A methodological approach to superoxide-dismutase (SOD) activity assay based on Inhibition of nitroblue tetrazolium (NBT) reduction. Clin Chim Acta. 1993;214(1):103–4.
34. Senthilkumar M, Amaresan N, Sankaranarayanan A. Estimation of Peroxidase (POD). In: *Plant-Microbe Interactions: Laboratory Techniques.* Edited by Senthilkumar M, Amaresan N, Sankaranarayanan A. New York, NY: Springer US; 2021:123–125.
35. Aebi H. [13] catalase in vitro. Methods in enzymology. Volume 105. New York, NY, USA: Academic; 1984. pp. 121–6.
36. Yang J, Cao Y, Zhang N. Spectrophotometric method for superoxide anion radical detection in a visible light (400–780 nm) system. Spectrochim Acta Part A Mol Biomol Spectrosc. 2020;239:118556.
37. Sedmak JJ, Grossberg SE. A rapid, sensitive, and versatile assay for protein using coomassie brilliant blue G250. Anal Biochem. 1977;79(1–2):544–52.
38. Wang Y, Yu Y, Zhang H, Huo Y, Liu X, Che Y, Wang J, Sun G, Zhang H. The phytotoxicity of exposure to two polybrominated Diphenyl ethers (BDE47 and BDE209) on photosynthesis and the response of the hormone signaling and ROS scavenging system in tobacco leaves. J Hazard Mater. 2022;426:128012.
39. Kim D, Langmead B, Salzberg SL. HISAT: a fast spliced aligner with low memory requirements. Nat Methods. 2015;12(4):357–60.
40. Pertea M, Pertea GM, Antonescu CM, Chang T-C, Mendell JT, Salzberg SL. StringTie enables improved reconstruction of a transcriptome from RNA-seq reads. Nat Biotechnol. 2015;33(3):290–5.
41. Buchfink B, Xie C, Huson DH. Fast and sensitive protein alignment using DIAMOND. Nat Methods. 2015;12(1):59–60.
42. Jones P, Binns D, Chang H-Y, Fraser M, Li W, McAnulla C, McWilliam H, Maslen J, Mitchell A, Nuka G. InterProScan 5: genome-scale protein function classification. Bioinformatics. 2014;30(9):1236–40.
43. Kanehisa M, Goto S, Kawashima S, Okuno Y, Hattori M. The KEGG resource for Deciphering the genome. Nucleic Acids Res. 2004;32(suppl1):D277–80.
44. Ashburner M, Ball CA, Blake JA, Botstein D, Butler H, Cherry JM, Davis AP, Dolinski K, Dwight SS, Eppig JT. Gene ontology: tool for the unification of biology. Nat Genet. 2000;25(1):25–9.
45. Love MI, Huber W, Anders S. Moderated Estimation of fold change and dispersion for RNA-seq data with DESeq2. Genome Biol. 2014;15:1–21.
46. Vaezi AR, Ahmadi M, Cerda A. Contribution of raindrop impact to the change of soil physical properties and water erosion under semi-arid rainfalls. Sci Total Environ. 2017;583:382–92.
47. Zhang R, Zheng C, Zhu D, Wu P, Liu Y, Zhang X, Khudayberdi N, Liu C. Variation in sprinkler irrigation droplet impact angle on the physical crusting properties of soils. Agric Water Manage. 2023;289:108514.
48. Bindea G, Mlecnik B, Hackl H, Charoentong P, Tosolini M, Kirilovsky A, Fridman W-H, Pagès F, Trajanoski Z, Galon J. ClueGO: a cytoscape plug-in to Decipher functionally grouped gene ontology and pathway annotation networks. Bioinformatics. 2009;25(8):1091–3.
49. Shannon P, Markiel A, Ozier O, Baliga NS, Wang JT, Ramage D, Amin N, Schwikowski B, Ideker T. Cytoscape: a software environment for integrated models of biomolecular interaction networks. Genome Res. 2003;13(11):2498–504.
50. Gumus I, Seker C. Effects of fall-spring cement applications on soil physico-mechanical quality of seed bed and seedling emergence. Environ Monit Assess. 2024;196(2):169.
51. Laker MC, Nortje GP. Review of existing knowledge on soil crusting in South Africa. In: *Advances in Agronomy, Vol 155.* Edited by Sparks DL, vol. 155; 2019: 189–242.
52. Abiri R, Shaharuddin NA, Maziah M, Balia Yusof ZN, Atabaki N, Sahebi M, Azizi P. Quantitative assessment of indica rice germination to Hydropriming, hormonal priming and polyethylene glycol priming. Chil J Agricultural Res. 2016;76(4):392–400.
53. Geng Z, Dou H, Liu J, Zhao G, Liu L, Zhao N, Zhang H, Wang Y, An Z. GhFB15 is an F-box protein that modulates the response to salinity by regulating flavonoid biosynthesis. Plant Sci. 2024;338:111899.
54. Wang Z, Li X, Zhu X, Liu S, Song F, Liu F, Wang Y, Qi X, Wang F, Zuo Z, et al. Salt acclimation induced salt tolerance is enhanced by abscisic acid priming in wheat. Plant Soil Environ. 2017;63(7):307–14.
55. Sharma V, Prasanna R, Hossain F, Muthusamy V, Nain L, Das S, Shivay YS, Kumar A. Priming maize seeds with cyanobacteria enhances seed vigour and plant growth in elite maize inbreds. 3 Biotech. 2020;10(4):154.
56. Ali F, Qanmber G, Li F, Wang Z. Updated role of ABA in seed maturation, dormancy, and germination. J Adv Res. 2022;35:199–214.
57. Feng ZH, Lu GR, Sun M, Jin YY, Xu Y, Liu XL, Wang MM, Liu M, Yang HY, Guan Y et al. Comparative study of the priming effect of abscisic acid on tolerance to saline and alkaline stresses in rice seedlings. Agronomy-Basel. 2023;13(11):2698
58. Xiong Q, Ma B, Lu X, Huang Y-H, He S-J, Yang C, Yin C-C, Zhao H, Zhou Y, Zhang W-K, et al. Ethylene-Inhibited jasmonic acid biosynthesis promotes

mesocotyl/coleoptile elongation of etiolated rice seedlings. Plant Cell. 2017;29(5):1053–72.
59. Ogawa M, Hanada A, Yamauchi Y, Kuwahara A, Kamiya Y, Yamaguchi S. Gibberellin biosynthesis and response during Arabidopsis seed germination. Plant Cell. 2003;15(7):1591–604.
60. Cao L. Effect of different hormones on mesocotyl length in Oryza sativa L. Acta Agron Sinica. 2005;31:1098–100.
61. Liu B, Lin R, Jiang Y, Jiang S, Xiong Y, Lian H, Zeng Q, Liu X, Liu Z-J, Chen S. Transcriptome analysis and identification of genes associated with starch metabolism in *Castanea henryi* seed (Fagaceae). Int J Mol Sci. 2020;21(4):1431.
62. Monroe JD, Storm AR. Review: the Arabidopsis β-amylase (BAM) gene family: diversity of form and function. Plant Sci. 2018;276:163–70.
63. Li HX, Li XZ, Wang GJ, Zhang JH, Wang GQ. Analysis of gene expression in early seed germination of rice: landscape and genetic regulation. BMC Plant Biol. 2022;22(1):70.
64. Sharma KD, Patil G, Kiran A. Characterization and differential expression of sucrose and starch metabolism genes in contrasting Chickpea (Cicer arietinum L.) genotypes under low temperature. J Genet. 2021;100(2):71.
65. Mukherjee S, Liu A, Deol KK, Kulichikhin K, Stasolla C, Brûlé-Babel A, Ayele BT. Transcriptional coordination and abscisic acid mediated regulation of sucrose transport and sucrose-to-starch metabolism related genes during grain filling in wheat (*Triticum aestivum* L). Plant Sci. 2015;240:143–60.
66. Muñoz-Llandes CB, Martínez-Villaluenga C, Palma-Rodríguez HM, Román-Gutiérrez AD, Castro-Rosas J, Guzmán-Ortiz FA. Effect of germination on starch. Starch: advances in modifications, technologies and applications. Springer International Publishing; 2023. pp. 457–86.
67. Carianopol CS, Chan AL, Dong S, Provart NJ, Lumba S, Gazzarrini S. An abscisic acid-responsive protein interaction network for sucrose non-fermenting related kinase1 in abiotic stress response. Commun Biology. 2020;3(1):145.
68. Shen N, Wang T, Gan Q, Liu S, Wang L, Jin B. Plant flavonoids: classification, distribution, biosynthesis, and antioxidant activity. Food Chem. 2022;383:132531.
69. Zhang J, Cheng K, Liu XY, Dai ZC, Zheng LL, Wang YC. Exogenous abscisic acid and sodium Nitroprusside regulate flavonoid biosynthesis and photosynthesis of *Nitraria tangutorum* Bobr in alkali stress. Front Plant Sci. 2023;14:1118984.
70. Chen L, Guo H, Lin Y, Cheng H. Chalcone synthase EaCHS1 from *Eupatorium adenophorum* functions in salt stress tolerance in tobacco. Plant Cell Rep. 2015;34(5):885–94.
71. Yuk HJ, Song YH, Curtis-Long MJ, Kim DW, Woo SG, Lee YB, Uddin Z, Kim CY, Park KH. Ethylene induced a high accumulation of dietary isoflavones and expression of isoflavonoid biosynthetic genes in soybean (*Glycine max*) leaves. J Agric Food Chem. 2016;64(39):7315–24.
72. Su L, Lv A, Wen W, Fan N, Li J, Gao L, Zhou P, An Y. MsMYB741 is involved in alfalfa resistance to aluminum stress by regulating flavonoid biosynthesis. Plant J. 2022;112(3):756–71.
73. Machado Dutra J, Espitia PJP, Andrade Batista R. Formononetin: biological effects and uses– A review. Food Chem. 2021;359:129975.
74. Wang Y, Jiang W, Li C, Wang Z, Lu C, Cheng J, Wei S, Yang J, Yang Q. Integrated transcriptomic and metabolomic analyses elucidate the mechanism of flavonoid biosynthesis in the regulation of mulberry seed germination under salt stress. BMC Plant Biol. 2024;24(1):132.
75. Wang D, Mi T, Huang J, Zhou R, Jin Y, Wu C. Metabolomics analysis of salt tolerance of *Zygosaccharomyces rouxii* and guided exogenous fatty acid addition for improved salt tolerance. J Sci Food Agric. 2022;102(14):6263–72.
76. Mekawy AMM, Abdelaziz MN, Ueda A. Apigenin pretreatment enhances growth and salinity tolerance of rice seedlings. Plant Physiol Biochem. 2018;130:94–104.
77. Liu X, Ji P, Yang H, Jiang C, Liang Z, Chen Q, Lu F, Chen X, Yang Y, Zhang X. Priming effect of exogenous ABA on heat stress tolerance in rice seedlings is associated with the upregulation of antioxidative defense capability and heat shock-related genes. Plant Growth Regul. 2022;98(1):23–38.
78. Shafi A, Zahoor I, Mushtaq U. Proline accumulation and oxidative stress: diverse roles and mechanism of tolerance and adaptation under salinity stress. Salt Stress Microbes Plant Interactions: Mech Mol Approaches: Volume. 2019;2:269–300.
79. Guo X, Zhi W, Feng Y, Zhou G, Zhu G. Seed priming improved salt-stressed sorghum growth by enhancing antioxidative defense. PLoS ONE. 2022;17(2):e0263036.
80. Zhang M, He S, Qin B, Jin X, Wang M, Ren C, Cao L, Zhang Y. Exogenous melatonin reduces the inhibitory effect of osmotic stress on antioxidant properties and cell ultrastructure at germination stage of soybean. PLoS ONE. 2020;15(12):e0243537
81. Feng S, Yao Y-T, Wang B-B, Li Y-M, Li L, Bao A-K. Flavonoids are involved in salt tolerance through ROS scavenging in the halophyte *Atriplex canescens*. Plant Cell Rep. 2024;43(1):5.
82. Gao Q, Li X, Xiang C, Li R, Xie H, Liu J, Li X, Zhang G, Yang S, Liang Y, et al. *EbbHLH80* enhances salt responses by up-regulating flavonoid accumulation and modulating Ros levels. Int J Mol Sci. 2023;24(13):11080.

Publisher's note